

Chemistry and mineralogy of outcrops at Meridiani Planum

B.C. Clark^{a,*}, R.V. Morris^b, S.M. McLennan^c, R. Gellert^d, B. Jolliff^e, A.H. Knoll^f,
S.W. Squyres^g, T.K. Lowenstein^h, D.W. Ming^b, N.J. Tosca^c, A. Yenⁱ, P.R. Christensen^j,
S. Gorevan^k, J. Brückner^d, W. Calvin^l, G. Dreibus^d, W. Farrand^m, G. Klingelhoferⁿ,
H. Waenke^d, J. Zipfel^d, J.F. Bell III^g, J. Grotzinger^o, H.Y. McSween^p, R. Rieder^d

^a Lockheed Martin Space Systems, POB 179, MS S-8000, Denver, CO 80201, USA

^b NASA Johnson Space Center, Houston, TX 77058, USA

^c Dept. of Geosciences, State University of New York, Stony Brook, NY 11794, USA

^d Max Planck Institut für Chemie, Kosmochemie, Mainz, Germany

^e Dept. Earth and Planetary Sciences, Washington University, St. Louis, MO 63130, USA

^f Botanical Museum, Harvard University, Cambridge MA 02138, USA

^g Dept. of Astronomy, Space Sciences Bldg. Cornell University, Ithaca, NY 14853, USA

^h Dept. Geol. Sci. and Environ. Studies, SUNY Binghamton, Binghamton, NY 13902, USA

ⁱ Jet Propulsion Laboratory, California Institute of Technology, Pasadena, CA 91109, USA

^j Dept. of Geological Sciences, Arizona State University, Tempe, AZ 85287, USA

^k Honeybee Robotics, New York, NY 10012, USA

^l University of Nevada, Reno, Geol. Sci., Reno, NV 89557, USA

^m Space Science Institute, Boulder, CO 80301, USA

ⁿ Johannes Gutenberg-University, Mainz, Germany

^o Massachusetts Inst. of Technology, Earth, Atmos. and Planetary Sci., Cambridge, MA 02139, USA

^p Dept. of Earth and Planetary Sciences, Univ. of Tennessee, Knoxville Tennessee 37996, USA

Accepted 22 September 2005

Available online 7 November 2005

Editor: A.N. Halliday

Abstract

Analyses of outcrops created by the impact craters Endurance, Fram and Eagle reveal the broad lateral continuity of chemical sediments at the Meridiani Planum exploration site on Mars. Approximately ten mineralogical components are implied in these salt-rich silicic sediments, from measurements by instruments on the Opportunity rover. Compositional trends in an apparently intact vertical stratigraphic sequence at the Karatepe West ingress point at Endurance crater are consistent with non-uniform deposition or with subsequent migration of mobile salt components, dominated by sulfates of magnesium. Striking variations in Cl and enrichments of Br, combined with diversity in sulfate species, provide further evidence of episodes during which temperatures, pH, and water to rock ratios underwent significant change. To first order, the sedimentary sequence examined to date is consistent with a uniform reference composition, modified by movement of major sulfates upward and of minor chlorides downward. This reference composition has similarities to martian soils, supplemented by sulfate anion and the alteration products of mafic igneous minerals. Lesser cementation in lower stratigraphic units is reflected in decreased energies for grinding with the Rock Abrasion

* Corresponding author. Tel.: +1 303 971 9007; fax: +1 303 971 2390.

E-mail address: benton.c.clark@LMCO.com (B.C. Clark).

Tool. Survival of soluble salts in exposed outcrop is most easily explained by absence of episodes of liquid H₂O in this region since the time of crater formation.

© 2005 Elsevier B.V. All rights reserved.

Keywords: Mars; outcrop; Meridiani; chemical sediment; sulfate; kieserite; jarosite; rover; MER; Opportunity

1. Introduction

Since January, 2004, the NASA rover Opportunity has been investigating outcrop rocks in the Meridiani Planum region of Mars. The Meridiani region was chosen for rover exploration because of its mineralogical signature for hematite [1] and intriguing geology as seen from orbit [2]. After landing, it was quickly discovered that the outcrop materials are chemical sediments, strongly enriched in sulfate compared to previously encountered martian rocks and soils [3–6]. However, direct measurements show these chemical sediments also host non-salt silicate and Fe-containing minerals [3–5]. In this report, we seek to synthesize and interpret these results, in terms of constituent minerals and their distributions in these sediments.

2. Data set

The APXS data set for these analyses is that prepared for publication [7] and provides minor improvements in calibration over a partial set published previously [3], while the MB data also provide some minor refinement over previous publication [4]. The core in situ analytical suite consists of the alpha particle X-ray spectrometer (APXS), Mössbauer spectrometer (MB), and rock abrasion tool (RAT). Although APXS+MB+RAT comprise less than 1% of the mission's total data, these results have proven essential for constraining candidate geochemical processes, especially aqueous, that have operated in this region of Mars. Other essential contributors to this synthesis are the miniature thermal emission spectrometer (Mini-TES), microscopic imager (MI), and panoramic camera (Pancam) data sets.

The key in situ compositional data come from 19 outcrop targets at three crater sites where grinding by the RAT exposed material 3–7 mm below their surfaces. Microscopic imagery (MI) of these samples revealed textural differences and the presence or absence of spherules, vugs, and veins that document diagenetic processes, discussed in McLennan et al. [8]. Textural patterns and bedding relationships that provide important clues to local aeolian and aqueous environments are discussed in Grotzinger et al. [9].

The Mini-TES IR spectrometer has analyzed several portions of outcrop. Significant variations between individual members of outcrop are difficult to extract from these spectra which are, however, consistent with derivations of sulfate minerals from MB and APXS data. Use of the RAT to grind into rocks has been essential for obtaining a comprehensive compositional data set on outcrop chemistry. APXS results, and to a lesser extent MB analyses of unprocessed surfaces, are compromised by contamination by airfall dust, soil, detritus, sand, spherules, and possibly rock coatings, weathering rinds and/or leached zones.

2.1. Quality of the data set

The Meridiani Opportunity rover's APXS has achieved extremely good precision and has discovered several soil samples of quite similar composition. For example, the analysis of bright dust soil Hilltop–Wilson on sol 123 is nearly identical to that for MontBlanc–LeHauches (taken over 60 sols earlier and hundreds of meters distant), with nine elements the same within 2% relative to their concentrations and another six elements deviating by less than 6%. The figure of merit (see Section 3.3 below), F , for a chemical compositional match between these two soils was 94.7%. In contrast, the F score for their matching with Tarmac class of soils was only 65% and in the range of 30% for outcrop rock material. Pair-wise matches from among all 19 outcrop RATED samples typically score only 60–70%, occasionally up to 80% for the highest F scores. Outcrop sample Diamond–Jenness (Fig. 1) had two RAT measurements, which score 89% for matching (without Cl, Br). These examples demonstrate that differences between outcrop units reflect geochemical variations, not measurement uncertainty.

Identifications by the Mössbauer spectrometer of hematite and jarosite, and the counter-indications of low or no olivine or magnetite in these outcrop samples, are considered robust. However, as noted previously [10,4], “pyroxene” is a tentative identification by MB, which conceivably could be instead a ferrous sulfate (see Section 4.2.5 for evidence to the contrary for these samples). The component termed Fe₃D₃ could be a ferric oxide or possibly a ferric sulfate (e.g., schwertmannite).

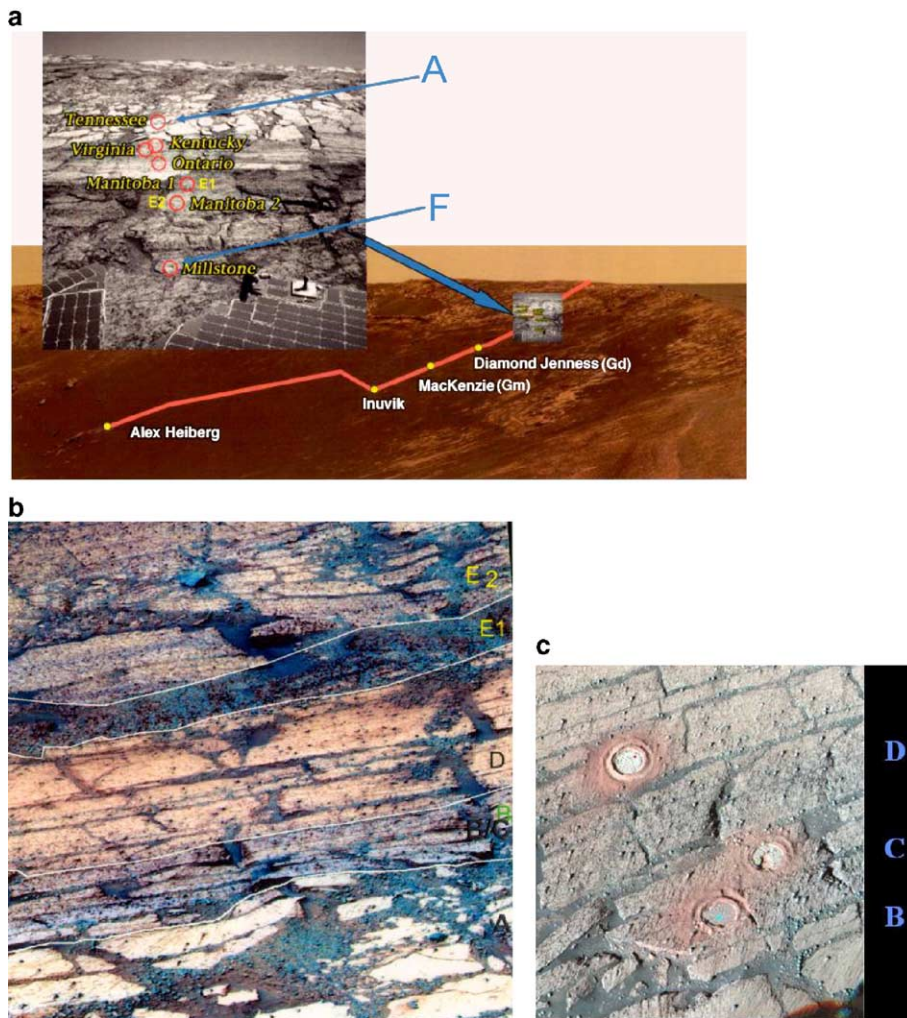


Fig. 1. Color images of the Karatepe outcrop sequence, showing the distribution of units A through G encountered and sampled during ingress at Karatepe West into Endurance crater. Units A through F define a stratigraphic succession in which F is the oldest and A the youngest unit. Table 1 provides specific correspondence between all names and letters. See Grotzinger et al. [9] for stratigraphic context and dimensions. (a) context image, (b) units A–E in false color, (c) units B–D in approximate true color. The images in (b) and (c) look downward into the crater, with stratigraphically lower units farther away.

These alternatives will be explored further below, by combining other data sets with the MB results.

3. Data analysis methodology

3.1. Element associations

Positive element associations could indicate their presence in a common mineral, or perhaps a common source for minerals that group together. Initial screening for such associations employs a search method that utilizes a scatter parameter, S'' , the value of which will be minimized when the variation of a ratio in actual samples (e.g., MgO/SO_3) is small compared to the

maximum variation it could reach based upon the range of values observed for the numerator (e.g., MgO) and denominator (e.g., SO_3). Mathematically,

$$R_{ij} = w_i/w_j, S_{obs}(ij) = \max(R_{ij})/\min(R_{ij})$$

where R_{ij} is the element ratio in a given sample for two elements of concentration w_i and w_j (in these and other calculations, we have chosen percent by weight (wt.%) as the unit of concentration), $S_{obs}(ij)$ is the observed scatter for the R_{ij} of all samples; and “min” and “max” are the operators which find the minimum or maximum measured values, respectively. Based upon the scatter in observed concentrations, the extreme in scatter, S_{ext} ,

that can occur for a particular ratio R_{ij} in the overall data set is given by,

$$\begin{aligned} S_{\text{ext}}(ij) &= (R_{\text{high}}/R_{\text{low}}), \text{ where } R_{\text{high}} \\ &= \max(w_i)/\min(w_j), \text{ and } R_{\text{low}} \\ &= \min(w_i)/\max(w_j) \end{aligned}$$

Comparing the observed scatter in ratios to the extreme scatter that could be observed, $S' = S_{\text{obs}}/S_{\text{ext}}$, and normalizing by the scatter that occurs in the reference element (j) alone, we define the “scatter parameter”,

$$S''(ij) = S'(ij)/S'(jj)$$

which has the property that it is 1.00 when two elements are both isolated to a single mineral or to a set of minerals whose relative proportions do not change.

3.2. Trend analysis

There are several pitfalls to element trend analysis. Errors in measurement accuracy inject noise into the data and may obscure trends. There can also be indirect effects. For example, consider the case of three independent components A, B, and C. If there is less of C in one sample, then elements in *both* A and B will indicate an increase even though there is no relationship between these two components. Trends in 2-axis plots will not be unique if one or both elements occur in more than two components that vary independently. In such cases, it is possible to have multi-valued results, which appear as scatter even when the measurements are error-free. Finally, the statistics of small samples and the uncertainties from incomplete data sets can sometimes produce spurious apparent trends. For this reason, we have chosen to include in these analyses only the 19 “interiors” of outcrop samples which were exposed by RAT grinding.

Data scatter in trends can also result from small-scale concentration variations. The variability of Br most likely reflects this type of heterogeneity. A second, even more subtle factor is physical heterogeneities which produce masking and so-called “matrix effects” in analytical methods. Differential composition with particle size at scales of microns to millimeters can lead to shielding effects which manifest as changes in X-ray intensities and hence calculated concentration levels. Salt-clastic mixtures are particularly prone to these effects in unprepared samples [11], because salt grain size is highly dependent upon aqueous history of the sample, while siliciclastic particle sizes may have resulted more from magmatic generation and aeolian transport processes. Relatively large salt crystals can be

partially masked by grains which adhere to them. Matrix effects such as “stealth salt” may not be a problem for these data because the analyses are restricted to samples after RAT grinding.

3.3. Compositional matching algorithm

Some outcrop rocks were encountered without stratigraphic context, such as LionStone at the rim of Endurance crater. To determine whether this float sample is truly different or may originate from a particular stratigraphic layer, we use a special algorithm that accounts for not only the actual element concentrations deduced from the APXS data but also the statistical errors in analysis. This algorithm is

$$F(n) = M_{n,o}/M_{o,o}$$

where $F(n)$ is a figure of merit for the match between the n th sample and the reference sample ($n=0$). The M factors are given by

$$M_{n,o} = \sum_i a_i \left[\left(\frac{|w_{i,n} - w_{i,o}|}{w_a} \right) + 3 \left(\frac{\varepsilon_{i,n}}{w_{i,n}} + \frac{\varepsilon_{i,o}}{w_{i,o}} \right) \right]^{-1}$$

where w_a is the mean concentration, $(w_{i,n} + w_{i,o})/2$, and $\varepsilon_{i,n}$ is the precision error in measurement of the i th element in sample n . A weighting factor of 3, rather than 1, is used to account for more than 1-sigma error in counting statistics and allow for additional potential non-systematic errors. The advantage of this algorithm is that it takes into account the $\varepsilon_{i,n}$ for the instrument [12,3] and objectively quantifies the match between two samples that are totally identical even though the reported data differ because of measurement errors. For the APXS instrument, these precision errors can be extremely small, as demonstrated above. To allow for tailoring of the criteria, a weighting function, a_i , with value of 0 to 1 is provided for each element or mineral component.

$F(n)$ can be expressed as a percentage because it has the property that it evaluates to 100% if the two samples are identical and the errors are the same for the two measurements or are vanishingly small. It evaluates toward zero if the two samples are mutually exclusive (e.g., magnetite vs silica) or the measurement errors of one or both samples are very large (avoiding false positives).

3.4. Mineralogical modeling

The goal of this work is to constrain the mineral makeup of the outcrop, which could then provide a basis for inferring the processes that have occurred in its formation and diagenesis. A total mineralogical

model is also necessary to clarify the more subtle contributions to trends. We have used the trends to infer candidate mineral assemblages, and from their likely compositions, to reconstruct the elemental composition for each member of the suite of samples. With this detailed, comprehensive model, it has been possible to vary the assumptions and test multiple hypotheses, as elaborated in Section 5.

4. Results

Within the interior wall of Endurance crater, a series of contiguous layers was mapped according to Pancam multispectral color and textural variations. Along the crater ingress route from a point designated Karatepe West, these layers were designated A through G, with A being stratigraphically highest and G lowest (see Fig. 1). Units E and G were each sampled twice, with distinctly different APXS results in both cases. These are designated as samples E1, E2, Gd and Gm. It cannot be precluded that sampling on a finer spatial scale would identify additional geochemically distinguishable layers.

4.1. Compositional stratigraphy

Moving down the Karatepe West outcrop sequence, the detailed composition varies significantly. Plots of eight elements are shown in Fig. 2. Using the algorithm given above for assessing compositional matches, we have evaluated the outcrop materials analyzed by APXS and MB at Eagle, Fram and Endurance craters, including those in the Karatepe A–G layers as well as individual

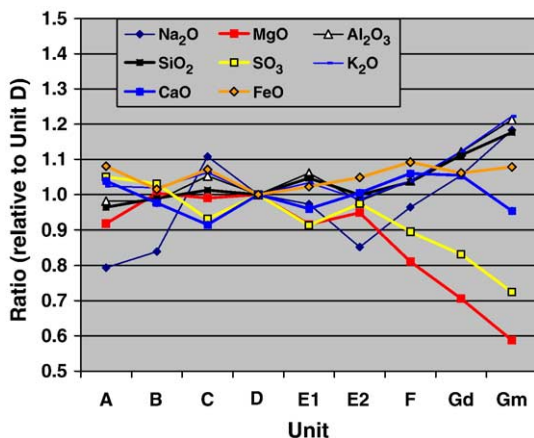


Fig. 2. Element trends with depth into the sequence at Karatepe, normalized to unit D (Ontario). The correlation and downtrend in Mg and S starting at E1 is apparent, as is the concordance between Al and Si. Anions Cl and Br, and trace elements (Zn, Ni) have larger variations, and are not shown for clarity.

Table 1

Figure of merit, F , for matches of all 19 RAT outcrop samples, taking Tennessee (A) as the basis unit

FOM (%)	Unit
100.0	Tennessee (A)
83.8	Fram Pilbara
67.3	Escher_Kirchner
64.7	Guadalupe (Eg)
60.2	Flat Rock (Eg)
56.6	Kentucky (B)
55.2	Manitoba Kettlestone (E2)
54.3	Millstone (F)
53.4	LionStone (End. Rim)
52.3	Ontario (D)
50.8	Virginia (C)
50.4	Diamond Jenness (Gd)
49.8	Paikea
45.9	Manitoba Grindstone (E1)
44.4	McKittrick (Eg)
41.9	Axel_Heiberg_Bylot
40.8	Wharenhui
39.1	MacKenzie (Gm)
32.8	Inuvik_Tuktoyaktuk
29.3	Bright Soil
28.5	Dark Soil
19.2	BounceRock

rocks and polygonally textured material encountered separately from this sequence. Although many of the variations are subtle, the compositional match algorithm typically provides significant discrimination among these samples. Most of the comparison screens use all sixteen elements ($a_1 = 1$), or remove only Cl and Br from the calculation ($a_{Cl} = a_{Br} = 0$). The latter are suspect because these two elements are hyper-variable relative to others. LionStone, from the rim of Endurance crater, matches best with layer D. The two rocks Inuvik and AxelHeiberg are more similar to nearby units Gd and F, respectively. Tabulation of matches relative to the reference unit Tennessee (A) is provided in Table 1. Here we see a good match with Fram, followed at some distance by Escher. The adjacent unit B is more significantly different from layer A than these several rocks from other locations. The outcrop rocks far down in the Endurance outcrop sequence are extremely poor matches to unit A and so are (as expected) the various soils. In Fig. 3, the order of samples preserves the stratigraphic layers as they were measured downward along the Karatepe outcrop sequence (A through G), but using the compositional match algorithm, the other outcrop samples have been merged among their most-similar specimens.

By this compositional algorithm, the Guadalupe outcrop at Eagle and the Pilbara rock at Fram both match best with Layer A (Tennessee) at Endurance. All three

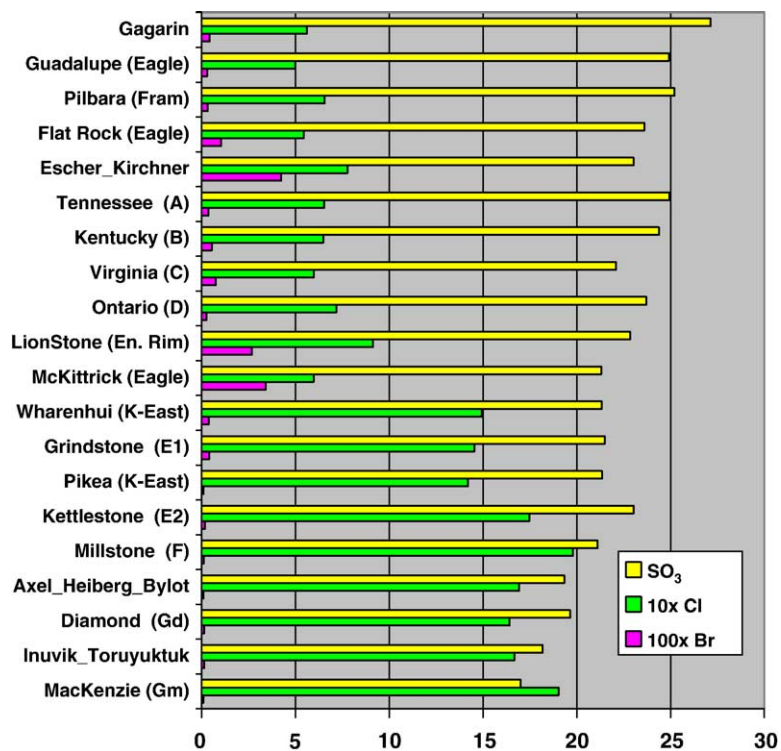


Fig. 3. Concentrations of measured salt-forming anions (S, Cl and Br). The list is ordered by stratigraphic location for Karatepe West samples (letters) and by similarity algorithm for all other samples. Samples are from Endurance crater, except those identified as from Eagle or Fram craters. Br and Cl concentrations are magnified (see Legend). The dichotomy in Cl concentration is clearly seen. Abscissa is weight percent for SO₃, and similarly for Cl and Br except multiplied by the factor given in the legend.

represent topmost layers in their respective craters. McKittrick, at Eagle, has its highest match scores farther down the sequence, with layers E1 and F. However, McKittrick has very high Br levels whereas the matched layers do not. Outcrop rocks in Eagle crater show evidence of local faulting, which may have placed stratigraphically distinct beds in topographic juxtaposition. FlatRock, from Eagle, matches Escher in Endurance slightly better than layer A. Escher best matches layer A, even though it has the highest Br concentration in RAT samples at Meridiani, while the Br of layer A is a factor of 17 less.

The result that the three craters have outcrop materials with identifiably corresponding chemistries across distances of hundreds of meters lends credence to the idea that those portions of the Meridiani Planum region with geomorphic similarity over the hundreds-kilometer scale could represent a widespread sediment formation [2,13,6].

4.2. Minerals

Thermal emission spectra obtained by Mini-TES have been used to derive the relative abundances of

several classes of minerals for Guadalupe [5], Pilbara, and an average of three different outcrop spectra at Karatepe in Endurance crater. In addition to a mixture of Mg and Ca sulfates and hematite, the samples contain a high-silica component modeled as glass/feldspar/sheet silicates (~35–45%). Crystalline silica minerals (e.g., quartz) and carbonate phases are not present in these outcrops at abundances >~5%. Minor jarosite is detected by Mini-TES.

From Mössbauer, two Fe minerals were identified with certainty in outcrop matrix: jarosite and hematite (Hm) [4]. None of these outcrop MB measurements included spherules in the MB field of view. Average outcrop matrix has 39 ± 6 wt.% of the Fe present as hematite.

Fe content of the spherules is not fully constrained because the spherule-rich targets contained significant open area within the fields of view of the instruments, with background materials which included the outcrop rock itself, airfall dust, and dark grains which may be basaltic sand. Careful measurements were made of relatively clean outcrop rock (BerryBowl_Empty) to facilitate differencing of spherules and their matrix. On this basis, the spherules are at least ~50% hematite [3,14,8,15].

Additional approaches for assessing the extent to which various minerals might be present rely on analyzing element trends and relationships, combined with geochemical plausibility based upon natural occurrences, likelihood of source material, and certain constraints of chemical kinetics and mineral stability fields. For example, for jarosite the specific variety (ferric hydroxide sulfates, with variable proportions of sodium, potassium, or hydronium as the univalent cation) is indicated by the MB measurements to be rich in Na and K, but by APXS to not correlate with these elements (see Section 4.2.5).

Element variability across all outcrop samples is restricted to a modest range for most elements, with Si, Al, Fe, P and Ca varying by less than 25% among all samples. S, however, rises to as much as 50% above the minimum amount found so far in outcrop. We note that the two most abundant oxides, SO_3 and SiO_2 , anticorrelate, as has been consistently shown also for martian soils [16]. The geochemical reasonableness of this is the paucity of minerals containing both Si and S, as well as abundant evidence for the presence of sulfate salts in both soils [17] and outcrop [5,4]. Because both are major components in outcrop, it is not surprising that the percentage abundance of one component decreases at the expense of increases in the other. Either S or Si could be taken as our reference point, but since the most striking features of the outcrop are those that indicate it is a chemical sediment [3,6], we chose to root our analysis relative to S (or, to be exact, relative to SO_3 because we report these results in terms of equivalent oxides of the elements). Although this may seem to imply the acceptance of this sediment as being fundamentally a “dirty evaporite,” it can just as well be viewed as a brine-infiltrated silicic sediment. In either case, alteration of some primary mineral phases that were originally in the silicic material has occurred, as discussed below and elsewhere [8].

For our mineralogical models, we have attempted to systematically derive a fixed suite of plausible minerals which, by varying their relative amounts, can reproduce the element and Fe-mineral trends as observed in the measurements made to date. Although there are no a priori data that prove this should be possible, the proximity of layers with quite similar compositions is justification for investigating this scenario.

First, we must look at individual trends in order to deduce a reasonable mineral assemblage to populate the model. To do this, we have examined correlations among 20 values, made up of all 16 elements measured by APXS and the four main iron minerals assayed by MB in the outcrop samples (hematite, jarosite,

“pyroxene”, and “ Fe_3D_3 ”). Pair-wise ratios have been examined for constancy (e.g., does MgO/SO_3 remain relatively constant, as it would if both elements were primarily present as MgSO_4 ; similarly, constant Al/Si could indicate aluminosilicates). Evaluating the S'' defined above for a large number of element ratios, the cases in Table 2 provided the lowest values.

Similar results were obtained with a correlation matrix, but with different relative importance. Inspection of trend plots of these pairs indicates, in most cases, that the elements in question associate together. The three most significant groups are (1) Si-group: Si, Al, Na, K, P; (2) S-group: S, Mg (nothing else is obvious, but see discussion on Ca); and (3) Fe-group: Fe, Ti, Cr, Ni.

In Fig. 4, as the S-group increases in relative concentration, both the Si-group and Fe-group concentrations decrease. Some or all of this effect is simply a result of “dilution,” because the sum of all oxide components has been normalized to 100% for each sample.

Identification of other group associations was attempted, but generally was not fruitful. For example, Cl, Br and Mn did not correlate positively with any other elements.

4.2.1. Si-group associations

Within the Si-group, the Al and alkali element correlations are particularly strong. The Al, K, Na and P concentrations closely follow Linear Least Squares (LLS) fits to the data with SiO_2 . For the aluminosilicates, the Al/Si slope extrapolates to a finite level of SiO_2 when Al_2O_3 is zero, indicating the presence of non-aluminous silicates such as pyroxene and/or silica. These trends also suggest that Al is exclusive to Si, and considerations below show that alternative interpretations are also counter-indicated. Although phyllosilicates have long been proposed for Mars, evidence in favor of this hypothesis remains minimal [18,19]. K and Na correlate positively with the concentration of Al (shown in Table 2), and the possibility that unweathered feldspars may exist in these outcrops must receive due

Table 2
Promising ratios from lowest scatter parameter (S'')

Ratio		Scatter parameter
Numerator	Denominator	
Cr_2O_3	FeO	1.024
K_2O	Al_2O_3	1.046
Na_2O	Al_2O_3	1.063
Al_2O_3	SiO_2	1.107
K_2O	P_2O_5	1.146
MgO	SO_3	1.184
TiO_2	FeO	1.185

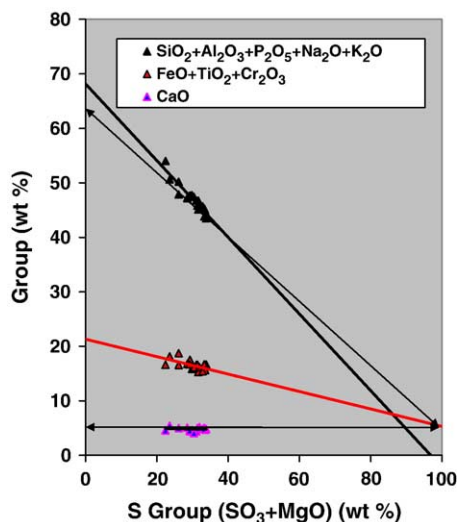


Fig. 4. Major groups of elements correlate with one another, but do not correlate positively with elements of other groups. Lines are LLS fits to data points, except for double-arrow indicating alternative trend.

consideration. If Na were partly taken up as NaCl, then the excess Na might correlate even more positively with Al, but this is not the case. Since the molar ratios of XO/Al_2O_3 are fixed for end-member feldspars at 1:1 (modal examples of Or, Ab, An), it is straightforward to evaluate the possible contributors for $X=K_2, Na_2$ and Ca. Stoichiometric mass balance indicates that even if both alkali elements are in feldspar, they are insufficient by a factor of two. The Al content is sufficiently high that one-third to nearly one-half of the CaO, depending on the specific sample, would be needed in plagioclase. However, Ca is likely the most complex and diverse of the elements in its partitioning between multiple mineral phases, as discussed below. This implies the possible presence of more aluminous alteration products, such as allophane, alunite or certain phyllosilicates, such as kaolinite.

Within all 19 outcrop RAT samples, the Al_2O_3/SiO_2 ratio stays remarkably constant at 0.163, within $\pm 4\%$ relative deviation, except for one modest outlier, Inuvik. This ratio is lower than in Meridiani bright and dark soils (dark soils by about 18%) and less than in Bounce rock and Gusev olivine basalt [21] by about 25–30%. Relative to aluminum, the outcrop is significantly more siliceous than its nearby surroundings. However, this is not the case generally if compared to martian meteorites such as the SNC classes [20], which could be more representative compositions for source material for the outcrop. Zeolites are unlikely because the alkaline conditions necessary for their formation run

counter to the acidic conditions inferred from other data (see below).

4.2.2. Sulfates

Martian soils are rich in S compared to those on Earth, Moon or meteorite parent bodies. Using a variety of constraints, it has been previously argued that the chemical form of S in soils is sulfate, not sulfide [22]. Likewise, the outcrop materials appear to be rich in sulfates, based upon Mini-TES spectra and MB detection of the ferric sulfate jarosite [4].

On Earth, the alkali elements Na and K, along with Cl, typically play a major role in evaporite deposits. At Meridiani Planum, the data indicate otherwise. In Fig. 5a, it is seen that Na is not positive correlated with SO_3 . Mg is well-correlated up to an SO_3 concentration of 22 wt.%. Ca reveals no preference, being highly conserved across all outcrop compositions. Stoichiometry places strong constraints upon which elements could provide the necessary cations for the abundant salt anions — sulfates, chlorides, phosphates, and potentially carbonates and nitrates. Constructing an ionic balance, the alkaline earths provide sufficient cation neutralization for the amounts of SO_4^{2-} , Cl^- and PO_4^{3-} . No single candidate cation is adequate, but Mg and Ca are sufficient in combination, as shown in the example of Millstone (layer F) in Fig. 6. For all outcrop samples, the combined Mg and Ca concentrations are adequate to balance all sulfates (other than the sulfate in jarosite, which is balanced by Fe^{3+}), plus all chlorides and phosphates, within cumulative measurement uncertainties. That Ca does play a role in sulfate minerals is indicated in Fig. 7, where it is seen that although bulk SO_3 anti-correlates with CaO, the residual SO_3 beyond that accounted for by jarosite and full use of MgO to form $MgSO_4$ does trend positively with CaO.

There are no obvious trends of Ca with virtually any other measured element. However, we believe that this may be misleading and could result from the fact that Ca occurs in many different minerals which, over the range of observation, happen to sum to a near-constant value. Alternatively, one could view this system as closed with respect to Ca, in effect isochemical with its source ingredients. However, the larger variations among all other elements provide evidence that this system is not fully closed. Obscured associations for Ca are not necessarily surprising because it is such a highly versatile element. Calcium occurs in common evaporite salts (sulfates, carbonates, and even chlorides and nitrates) and is the almost universally preferred species in nature to complex with phosphates (in

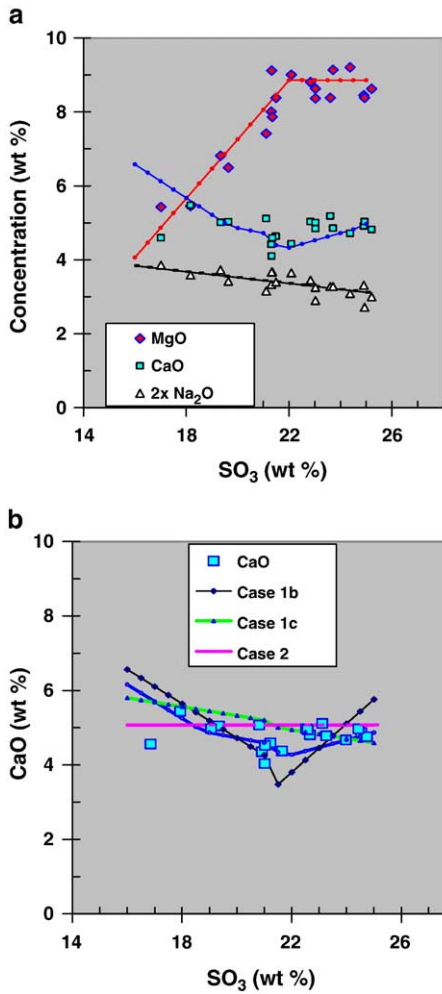


Fig. 5. Model calculations and measurements for candidate salt cations. Note the simulated exhaustion of MgO, and the difficult and imperfect match in CaO components. The downward slope of Na₂O is primarily due to the dilution effect. (a) Case 1a. (b) Cases 1 and 2 models for CaO data points vs SO₃. The solid blue line is case 1a.

some highly weathered materials, Al is associated with P). In igneous provenances, Ca is also a ubiquitous element, playing a prominent role in mafic minerals, such as pyroxenes, and in feldspars, such as anorthite. Ca for salt compounds would be expected to have come from source Px or plagioclase. Experience in terrestrial weathering, laboratory experiments [22–24] and theoretical analyses [25] shows that igneous glass and olivine minerals are preferentially subject to alteration compared to more resistant minerals, including augites and plagioclase.

Experimental [26] and observational examples of acid sulfate alteration in basaltic and pyritic terrains [27,28] frequently produces Al–sulfates. In the Meri-

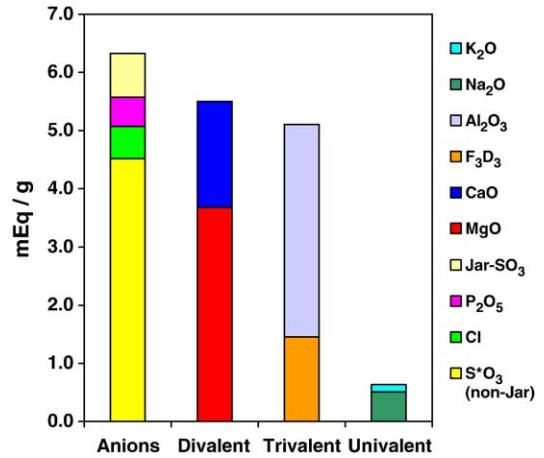


Fig. 6. Ion balance for candidate anions (column 1) and cations (columns 2–4) in the Millstone (*F*) outcrop. Mg and Ca cations could be sufficient for all the sulfate (non-jarosite), chloride and phosphate anions, combined. The univalent cations are clearly inadequate for sulfates. Trivalent ions are potentially sufficient, but element trends do not support this (see text, Section 4.2.2). Units are milliequivalents per gram.

diani outcrop, Al has a strong anti-correlation with S which implies only small or no contributions from Al–sulfates (e.g., alunite, natroalunite, or alunogen).

An intriguing but conceptually difficult possibility is that the missing but required cation neutralization is supplied not by Ca²⁺, but rather by H⁺. This would simplify the mineralogical model (see Section 5.1.1 below), but imply that Meridiani outcrop contains

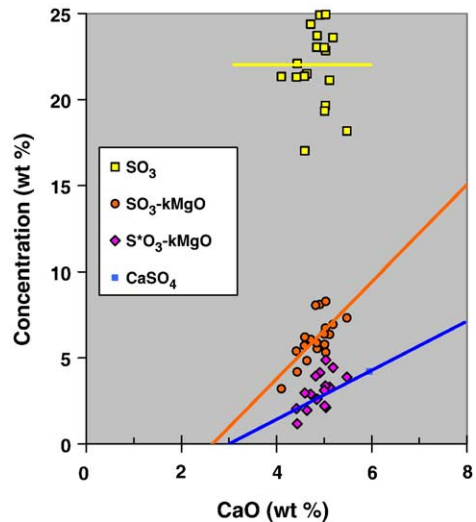


Fig. 7. Ca does not correlate with bulk S (top points). However, subtractions of SO₃ equivalent to all MgO as MgSO₄ (*k* 1.986) from bulk SO₃ and from S*O₃ (the SO₃ after subtraction of jarosite-SO₃), reveal positive correlations with CaO. Slopes are somewhat steeper than the ideal slope for pure CaSO₄.

unreacted sulfuric acid. Under the cold, dry conditions on contemporaneous Mars, this is marginally plausible, but over geologic time and with obliquity variations that could markedly alter the temperature and water activity [29,30], including the possibility of tropical ice, this seems unlikely. However, the mere presence of highly soluble salts in exposed outcrop slopes attests to the lack of significant water activity since crater formation. Abrasion pH's [31] of the common igneous minerals are almost universally alkaline. For example, olivines and pyroxenes typically equilibrate at pH 10 to 11, anorthite at 8, and carbonates over a range of alkalinity up to 12, depending on the cation composition and atmospheric CO₂ levels. However, in view of the knowledge that jarosite has formed at least in the past, residual acidity is difficult to rule out at this time. If so, this mandates that carbonates and at least some nitrates cannot concurrently be present [32], but likewise that amounts of H₂O sufficient to promote neutralization reactions with less reactive components has been extremely limited for the past billions of years. On Earth, jarosite commonly includes alkali elements. However, Fig. 8 shows that K is insufficient to account for stoichiometric K-jarosite. There is adequate Na, even if a portion of it is tied up in chloride, to form natrojarosite but the data are scattered and do not reflect the expected trend. Since evidence presented above shows the likely location of Na and K in an aluminosilicate, this independent result is not surprising. Al-

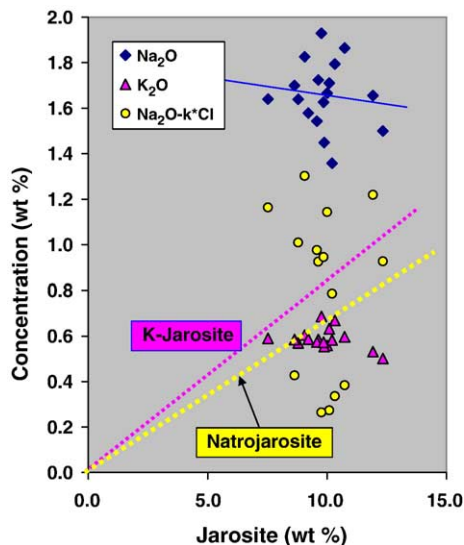


Fig. 8. Potassium is at inadequate concentration for the common form of jarosite (dotted line, “K-jarosite”) in these outcrop materials. Na₂O is at a sufficient level to form natrojarosite, with more than 0.5 wt.% excess, but the data do not conform to the expected trend lines, even when corrected for Na in NaCl. Hydronium jarosite may be indicated.

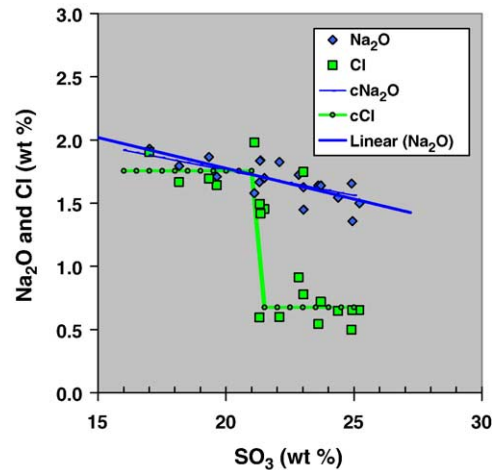


Fig. 9. Modeled Cl assumes a step function in occurrence. Na is modeled for correlation with Al, yet matches the observed Na trend even with apparent pseudo-correlation with Cl up to SO₃=21%. Heavy blue line is LLS fit to Na trend; cCl and cNa₂O are values calculated from the mineralogical model (Case 1a).

though the theoretical thermodynamic calculations of Tosca et al. [25] predict that hydronium jarosite is the predominant form of this mineral, (Na, K)-jarosite is indicated by the MB spectral details.

4.2.3. Halides

In searching for evidence of differential salt precipitation or dissolution, it was noted early-on that S, Cl and Br are decoupled in the first two outcrop measurements [12,6], Guadalupe and McKittrick. Subsequent measurements have reinforced this conclusion, as seen in Fig. 3 where Cl enrichments have been discovered in layers E1 through G of the Karatepe sequence, whereas Br is low or undetected. Combining all outcrop data, the plot in Fig. 9 shows a general anti-correlation of Cl with S, but especially as evidenced by two distinct clusters of Cl concentrations, with the more abundant group having on average twice the Cl concentration as the other group. This Cl dichotomy has considerable potential diagnostic interest, and might also be used to attempt to identify the chloride cation(s). When we utilize NaCl for chloride in our mineralogical model, it predicts significant discrete jumps in the Na concentrations, which are not apparent in the data. In Fig. 10, the much stronger correlations of Na with K and Al than as expected with Cl for NaCl are revealed. K is not adequate for Cl, so the next likely candidates are Mg, Ca, or Fe. All three of these correlate flat or negatively with Cl, but this could reflect their association with other elements and the fact that Cl generally anti-correlates with S.

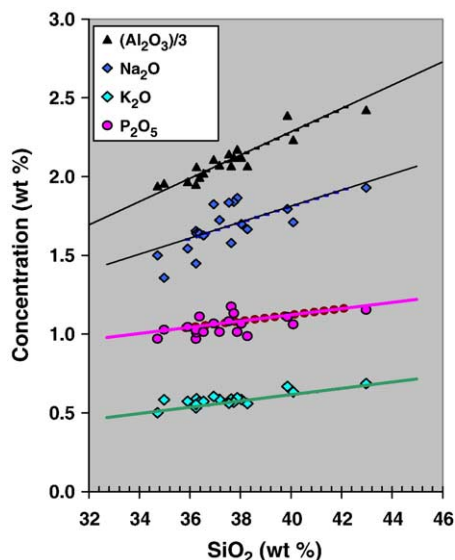


Fig. 10. Model (case 1a) comparisons between SiO_2 and oxides of elements Na, Al, and K.

Searches were conducted for samples as similar as possible but with major differences in bromine or chlorine. For example, Escher, with 547 ppm Br, and Tennessee (A) with 32 ppm, are otherwise quite similar in elemental compositional profile. Likewise, pair-wise matches of E1-to-McKittrick and D-to-LionStone also have order of magnitude differences in Br. Careful comparisons were unable, however, to reveal which cation might be involved with Br. This is not surprising because the absolute change in Br is less than 0.05 wt.%, and the likely cations are already present at levels one to two orders of magnitude higher than this, so that small changes could be hidden within measurement uncertainties. Bromine enrichment can occur in late-stage precipitation since Br is largely excluded from substituting in the halite crystal structure. Br is accommodated at higher concentrations in many other Cl minerals, such as sylvite, bischofite (Mg–chloride 6-hydrate), tachyhydrite, and hibbingite [33]. Interestingly, Br is strongly enriched in association with sulfate-rich brines in several disparate occurrences on Earth [34,35]. Br on Mars also occurs in duricrusts at Chryse [11], deep trenches at Gusev [12], and some coatings and soils. The hyper-variability and erratic pattern of these occurrences has led Yen et al. [16] to hypothesize other vectors of concentration, such as frost formation with possible dependencies on orientation with respect to solar insolation.

A similar search for Cl cation identification was conducted. In general, most high-Cl outcrop rocks (layers E1–G, where the Cl enrichment is strong) cor-

respond more closely to one another than to low-Cl rocks. However, three pairs: E1/McKittrick, E2/FlatRock, and F/McKittrick, looked promising. When examined carefully, these pairs indicated that Mg or Ca may be involved as chlorides, although not to the same degree for each sample. In contrast, Na, K and Fe differences have neutral to negative correspondence with Cl changes in all three cases. The situation with Na is particularly uncertain, however, because its X-ray is the lowest energy analyzed by the APXS instrument. The majority of the signal for Na emanates from the first one micron of depth into the sample, and is thus particularly susceptible to attenuation or masking by surficial stains. Statistics are poorer for Na than for other light elements because of lesser concentration and lower detector efficiencies. Finally, because the Na peak is contiguous with the low-energy cutoff of the instrument, it is uniquely sensitive to temperature corrections made to the spectra.

Another alternative and undetectable cation would be Li^+ . Enrichment of this alkali element is noted particularly under conditions of hydrothermal activity [36], but accompanying patterns of other enrichments are not evident in these data. Furthermore, to proxy for Mg^{2+} and Ca^{2+} in achieving ionic balance for Cl would require high values of Li, 700 to 2700 ppm.

4.2.4. Atypical salt assemblages

Finally, it should be noted that the conventional assumption that Cl implies chlorides could be incorrect. Highly oxidized conditions persist at the martian surface, as evidenced by strong, photochemically generated oxidants in the atmosphere [37,38] and soils [39]. Oxidizing conditions are also implicated for the past, at least at the time of jarosite formation [24,4,25]. Although uncommon on earth, other forms of Cl-salts should be considered, including the chlorites, chlorates and perchlorates. Magnesium perchlorate, $\text{Mg}(\text{ClO}_4)_2$, is well-known as a drying agent because of its strong deliquescence in forming the 6-hydrate. Perchlorates have been found, associated with nitrates, in the Atacama Desert [40]. Bromates and pyrosulfates may be present. All these compounds are highly soluble like their less-oxidized counterparts [41], and their oxidizing power could suppress formation or persistence of organic matter in martian regolith.

4.2.5. Systematics of Fe-group minerals

“Px”, as detected by the Mössbauer spectrometer, is the Fe-bearing component tentatively identified as pyroxene. In a typical augite, FeO constitutes about 15% of the composition. However, various other pyroxenes

can contain more or less Mg, Ca, or Fe, which also affect the Si and Fe content. To attempt to verify and understand this component, we examined the variation in these elements versus “Px”. Both Fe and Si correlate positively with “Px”, which is expected if this component is pyroxene mineral(s). S correlates negatively, which indicates that one alternative candidate, a ferrous sulfate, is not likely. This is consistent with the generally oxidizing martian environment considering the easily oxidized nature of this salt. Ca is invariant with “Px”, but Mg shows a slightly negative correlation. Since “Px” is less than one-tenth of the total mineral assemblage, however, it is possible that variations in other minerals are dominating these trends.

A number of elements either have associations with Fe, or potentially could serve as substitutional atoms in iron minerals. For example, outcrop Cr shows a clear trend with Fe. This is driven mainly by correlations with Hm and “Px”, whereas the Cr correlation is weak or negative with Fe_3D_3 and jarosite. Cr is well-known to occur at significant levels in some pyroxenes. This same result is found for some other elements, including Ni and to some extent Al. In general, jarosite is flat or strongly negative with nearly all elements, yet varies significantly within the outcrop ($1.6\times$ for min:max concentrations). The average jarosite abundance by MB combined with APXS is just over 10 wt.%. Given the low spectral contrast of this outcrop, this value is consistent with a marginal detection of jarosite by Mini-TES. As such, it may be an independent component. Incorporation of Al is a distinct possibility, both in pyroxenes and in Fe^{3+} minerals, including jarosite and hematite. Trend plots show weak positive correlation of Al with Hm, but questionable association with “Px” and Fe_3D_3 , and clear anti-correlation with jarosite. On the other hand, Hm correlates strongly with total Fe. It also is somewhat positive with Si (more so than is any other Fe mineral), which is consistent with association with the siliciclastic components, perhaps as an alteration coating on some grains. The Fe_3D_3 component is slightly negative with S, ruling out coquimbite, but not sufficiently to rule out schwertmannite because of that mineral’s relatively low SO_3 content. Both these minerals are found in the Rio Tinto sequences [27].

Ti has previously been found to correlate with a fraction of Fe in martian soils [11,42,12,16]. In outcrop, Ti shows a weak positive correlation with all MB Fe minerals, except jarosite. Overall, as before, the indication is that only a portion of the Fe minerals include Ti. Accordingly, anatase (TiO_2) might be present.

4.2.6. Other elements and minerals

Mn and Zn correlate with almost no other elements, except for indications of association of Zn with a portion of the Ca (but not with P). It is notable that whereas Mn occurs at similar concentrations in all known martian materials, Zn is markedly higher, by a factor of 5 or more, in soils and outcrop [12,3] than in martian igneous rocks (including martian meteorites [35]). This high Zn could be a byproduct of volcanic emissions [43,36]. A pyroclastic origin for some or most outcrop material is a possible extension of this observation.

4.3. Surface chemical alteration

Relatively little information has been obtained to date on the possibility of alteration of the surfaces of exposed outcrop materials. However, in several instances undisturbed rock surfaces were measured prior to RAT grinding. In addition, the rock Escher, which as shown above has chemical concordances with the topmost outcrops in all three craters, was studied with brushing prior to RAting. These samples allow us to test the hypothesis that outcrops have an exogenous coating or a surficial weathering zone different in composition from unaltered materials beneath. An additional consideration is whether airfall dust or saltating soil grains contaminate the outcrop surface. Dark grains are seen on some outcrop surfaces by microscopic imagery (MI), but micron-sized dust particles are far below the $100\ \mu\text{m}$ resolution limit (3-pixel criterion) and would not be apparent, except perhaps as a soil-mimicking coloration over the light colored rocks. Because of the low penetration of APXS fluorescent X-ray emissions, even such small grains can cause significant attenuation. Soft X-rays, especially for the light elements (Na, Mg, Al, Si, P), will emanate from the dust grains but those from the deeper outcrop material will be absorbed. Although the full analysis is significantly more complicated, a useful first approximation is to assume that the fractional areal coverage of dust and rock produce an arithmetic composite spectrum and element analysis. Calculations for Escher show that with a fractional area of 0.47 of soil (taken as the average of Tarmac and Mills-Dahlia soils) compared to the interior composition obtained after a RAT grind, the “as is” analysis has the same result for S and within 1% to 6% of the correct concentrations of Mg, Al, Si, Ca and Ti. However, Na and Cl are much higher than predicted. Similarly, after brushing, the resulting composition can be explained by a “residual contamination” of 0.39 areal coverage by soil. Although this fractional coverage is surprisingly high, the RAT brushes used for this procedure were not designed for cleaning rough

surfaces of micron-sized dust, but rather for removing chips and grains from ground surfaces. This degree of coverage is consistent for explaining the observed S and elements listed for the “as is” case. Na and Cl are still elevated (by factors of 1.3 and 1.6, respectively) above this simple prediction. K is higher by 1.1. These results implicate a chloride salt coating, reminiscent of the type that has also been found on the rock Mazatzal in Gusev crater [12,44,45]. In both locations, it is not known whether the Cl is derived from the surrounding soil or from the substrate on which it exists. A caveat is that Escher is near the Cl-rich lower part of the Karatepe sequence and could have its surface contaminated. Although it might seem that the surfaces of outcrop are depleted in S by leaching of sulfates, this analysis shows that dust contamination is a reasonable explanation of the apparent deficiency of S compared to interior rock, but that chloride coatings may exist.

No evidence is seen, however, of the action of liquid water since excavation and exposure of outcrop material by the Endurance impact. Abundant liquid H₂O would have leached salts from at least the outer layers of the outcrops, and formed salt deposits in crater bottoms. Although such deposits might be obscured by dunes and dust, there is no evidence of salt-impoverishment beyond a millimeter or so into these outcrops. With their apparent porosity, as evidenced by low strength against grinding, the presence of vugs, and fine-scale granularity, leaching by runoff should have been more effective.

5. Mineralogical models

5.1. Hypothesis testing

procedure with some similarity to normative mineralogical protocols for igneous chemical compositions is used to develop the models for the mineralogical composition of the outcrop. Individual parameters are adjusted to obtain overall best fits to observed trends in the actual data. The starting reference points are: the total SO₃ concentration, which sets the level of sulfate anions but not the cations; the distribution of Fe according to linear least squares fits to the MB results; and element correlations as discussed above. Below, we describe cases that adopt differing assumptions.

5.1.1. Case 1

An aluminosilicate is assumed, with Al₂O₃/SiO₂ ratio appropriate to feldspar plus various alteration products. Adjustable proportions of Na, K and Ca are invoked in the aluminosilicate.

A particular pyroxene composition is assumed as a trial, and from its Mg content, plus that assumed in chloride, the MgSO₄ is calculated by an algorithm devised to match the strong observed linear Mg trend with S, until reaching a saturation plateau above SO₃=22.9 wt.%.

That amount of SO₃ not accounted for by jarosite and MgSO₄ is calculated as CaSO₄. Hydronium jarosite is assumed in the model example presented here, as implied by APXS data, although (K, Na)-jarosite is implied by the MB results. The type of jarosite does not affect its sulfate content since Fe₂O₃/SO₃ is the same for K, Na and H varieties.

Cl is taken as either a Mg or Ca chloride, or a combination of both, depending on the model, and can be toggled from a high to a low value, depending on the sample or on SO₃ content. In case 1, individual outcrop Cl measured concentrations are used.

P is converted to a Ca-phosphate, since primary whitlockite is common in martian meteorites and the Ca stoichiometry is also about the same for apatites as well as for phosphate leachates from martian meteorites, using weakly acidified (pH 3–6) solutions of MgSO₄ [46].

Finally, pyroxene composition is varied empirically at the end of the calculation to achieve best overall matches for its candidate cations. Silica is added as necessary to achieve final SiO₂ levels and a tailored “Ca–other” component can be used to help flatten the Ca trend. These two adjustments are interactive since “Px” levels are determined by the FeO content assumed and the MB measurements.

The model is quite sensitive to assumptions because Mg, Ca, Fe and Si may be contributed by three or more different minerals in different groups. It has been found generally possible to reproduce the trends among all the important element pairs with a preset assemblage of minerals, as shown in Figs. 5, 9–11. An example mineral relative abundance is shown in Fig. 12a, and the variations of modeled mineral content for the nine layers is shown in Fig. 13. In this case, all Ca is apportioned to the salts, but none is allocated to the aluminosilicate or pyroxene (see Section 5.1.2 below for an alternative model). In addition, for case 1a minor CaCO₃ is added between SO₃=20 and 24 wt.%, peaking at a level of 2.3 wt.% when SO₃=22.1%, to better match Ca values. This is well below the upper limit for detection of carbonates in outcrop by Mini-TES, and is in the range inferred for carbonates in martian dust [47]. In case 1b, no carbonate is assumed, which affects the Ca trend, Fig. 5b.

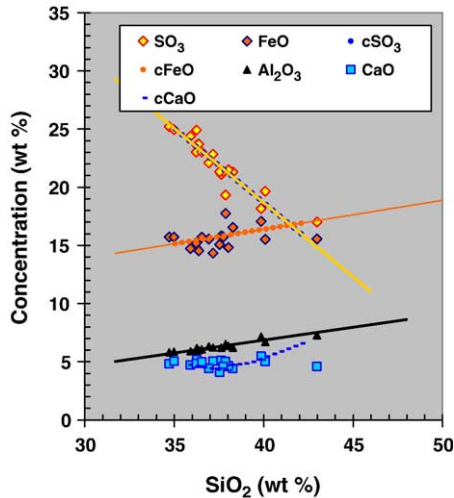


Fig. 11. Model results compare well with measured trends for major components, including the anti-correlation of SO_3 with SiO_2 . Lines derived from symbols with the “c” prefix are calculated from the case 1 mineralogical model.

Case 1c is a special assumption, which evades the difficult problem that Ca concentration does not trend linearly with other elements, by using unreacted H_2SO_4 (or, HSO_4^- on mineral surfaces) as a component. This allows the deficiency in Mg^{2+} to be made up by the H^+ cation in balancing the sulfate ion. It also permits Ca in the aluminosilicate and in pyroxene. Case 1c modeled trends of Ca are monotonic and may provide a somewhat better fit to the observations than for case 1a (Fig. 5).

5.1.2. Case 2

In this model, there is no hydronium jarosite but rather (K, Na)-jarosite as detected by MB, and excess Na after combining with Cl is included in thenardite (Na_2SO_4). Nanophase ferric oxide (np-Ox) plus schwertmannite are constrained by the MB results for the Fe_3D_3 doublet. Mg and Ca are associated with sulfate. Phosphate is aluminous rather than calcareous. A basaltic component, with composition taken from Bounce Rock, comprises 15–17 wt.% of the outcrop. This concentration is consistent with the Fe^{2+} doublet observed in the MB spectra. Al is modeled primarily as allophane with minor contributions in jarosite and np-Ox. The results of the calculation are given in Table 3 for water-free compositions, as appropriate for APXS results.

An important distinction between cases 2 and case 1 is that the former models most alkali elements and aluminum in alteration products, whereas the latter invokes feldspar combinations for Na–K–Al. Case 2

may help explain Ca systematics, Fig. 5(b). Interestingly, both approaches infer the major presence of low-Al silicates (modeled as silica plus allophane polymorphs) to the extent of one-fourth to one-third of the total assemblage, (Fig. 12). The unaltered rock components are somewhat lower in case 2.

5.2. Migration of soluble components

The mineralogical models for cases 1 and 2 show that their largest changes from layer to layer are in the Mg and Ca sulfates and in chlorides, and that they are systematic. We therefore tested a hypothesis that the Karatepe sequence could be explained as a single

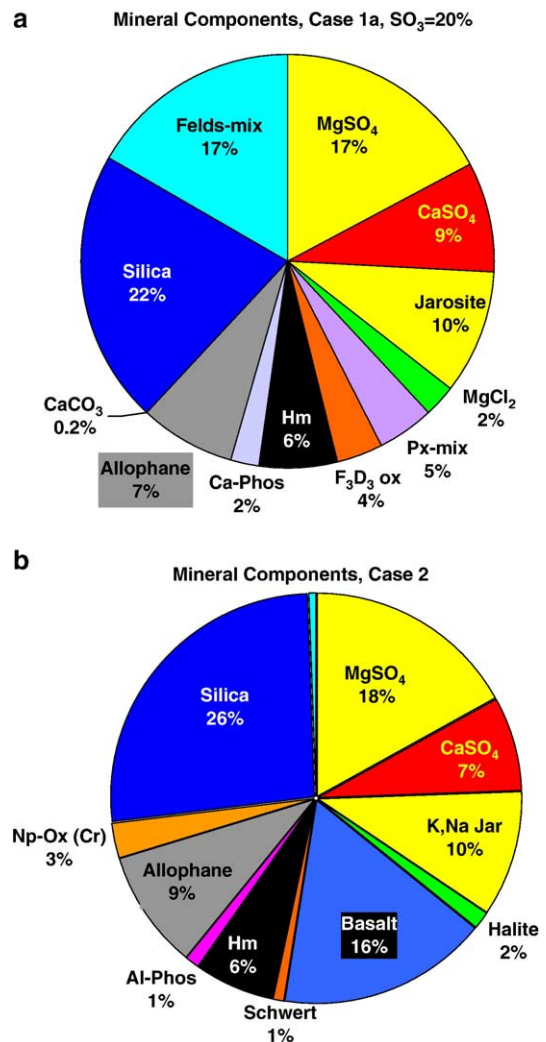


Fig. 12. Mineral components for modeled case 1a and case 2, for $\text{SO}_3=20.0$ wt.%. Although the two models incorporate several different assumptions (see text), their derivation of excess silica and partitioning of salts among cations is similar.

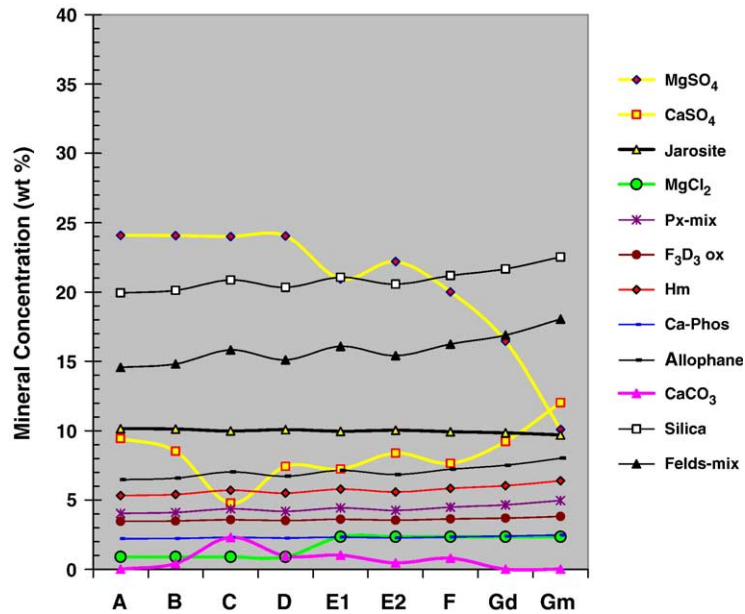


Fig. 13. Variations of modeled minerals in the Karatepe outcrop sequence, as deduced from the smoothed mineralogical model (Case 1a) and the specific SO_3 content of each layer.

chemical sediment, originally uniform in composition, but modified by migration of certain salts. In Fig. 14, we plot the composition of the hypothetical starting sediment, “reference composition” assuming movement of an average salt with the following composition: 90% MgSO_4 , 15% CaSO_4 , and -5% NaCl . The negative content for Cl signifies that as the sulfates are added, chloride is depleted. The relative constancy in the derived reference composition from each layer is in remarkable contrast to the compositional variations shown earlier in Fig. 2. Although the derived compositions still show residual systematic variations, these are small (within $\pm 10\%$ of the reference), lending credence that to first order the outcrop may be represented as one in which sulfates migrated upwards, while Cl and Na component(s) migrated downward. The “mobile salt” quantities used for this example are given in Table 4. Alternatively, the same salt differentials could reflect changes in deposition when salt-rich brines first infiltrated the siliceous sediment.

RAT grinding energies generally correlate positively with SO_3 content, and hence negatively with SiO_2 (BounceRock, an igneous rock at Meridiani, being the sole exception). However, the correlation with the calculated “mobile salt” shown in Fig. 15 is quite consistent with the expectation of increased cementation strength of salt-enriched sediments, in comparison with porosity and weakness of salt-depleted ones.

6. Implications

6.1. Source material

Compared to martian rocks and soils, outcrop compositional patterns are much more akin to soils, as is apparent by strong enrichments in S, Cl and Zn. However, the S content is markedly exaggerated. To examine the proposition that outcrop may simply be soil with addition of SO_3^{2-} , we have compared our derived reference composition for outcrop with Meridiani soils to search for components which could accommodate the differences. This approach is by no means unique, but to bracket some possibilities, we studied combinations with both the bright and dark soils analyzed at Meridiani, the former of which are particularly close to soil compositions across wide regions of Mars [16]. Adding a SO_3 -rich mixture containing mafic igneous minerals (or their isochemical alteration products) to dark soils, neither olivine nor pyroxene alone provide a good match, but a judicious combination of both is far more satisfactory. Similar results are shown in Table 5, where 66.6% bright soil is combined with 19.4% of a mix of volatiles, and 14% mafic component to reproduce the reference composition. The volatile component is predominantly S, with minor but significant P, Cl, K and Zn. The mafic component, of composition shown in Table 5, is 28% olivine ($Fo=59\%$ by wt.) and balance pyroxene ($En=55\%$ by wt., $Fs=38.5\%$, $Wo=6.5\%$). This mafic com-

Table 3
Mineralogical composition of outcrop cases (H₂O-free)

	Case 1a (SO ₃ =20%) (wt.%)	Case 2 (average) (wt.%)
<i>Rock component</i>		
Basaltic rock	0.0	16.2
“P _X ”	4.6	0.0
Feldspar (Ab=79% by wt., Or=21%, An=0%)	16.7	0.0
Sum rock component	21.3	16.2
<i>Oxide components</i>		
Hematite, Fe ₂ O ₃	6.0	6.0
Anatase, TiO ₂	(0.7)	0.6
Pyrolusite, MnO ₂	(0.3)	0.3
Np-Ox, (Fe _{0.94} Cr _{0.06}) ₂ O ₃ (Fe ₃ D ₃)	3.7	2.7
Sum oxide components	10.7	9.6
<i>Sulfate components</i>		
Jarosite, (K _{0.51} Na _{0.49})(Fe _{0.91} Al _{0.09}) ₃ S ₂ O ₁₁ (H ₂ O) ₃	0.0	9.9
H-Jarosite, (H ₃ O)Fe ₃ S ₂ O ₁₁ (H ₂ O) ₃	9.9	0.0
Schwertmannite (Fe ₃ D ₃), (Fe _{0.94} Cr _{0.06}) ₃₂ O ₆₉ S ₇ (H ₂ O) ₉	0.0	1.0
Kieserite, (Mg _{0.99} Ni _{0.01})SO ₄ (H ₂ O)	17.3	17.6
Bassanite, Ca(SO ₄)(H ₂ O) _{0.5}	8.8	7.4
Thenardite, Na ₂ SO ₄	0.0	0.5
Sum sulfate components	36.0	36.5
<i>Chloride components</i>		
Bischofite (MgCl ₂)(H ₂ O) ₆	2.4	0.0
Halite (NaCl)	0.0	1.9
<i>Phosphate component</i>		
Ca-phosphate	2.4	0.0
Variscite, (Al _{0.90} Fe _{0.10})PO ₄ (H ₂ O) ₂	0.0	1.2
<i>Aluminosilicate components</i>		
Allophane, halloysite, and/or kaolinite, Al ₂ Si ₂ O ₇ (H ₂ O) ₂	7.4	8.9
Opalline silica, SiO ₂ (H ₂ O) _{0.2}	21.5	25.8
Sum aluminosilicate component	28.9	34.7
<i>Carbonate component</i>		
CaCO ₃	0.2	0.0

position is in the range of various pyroxene-rich rocks, including the martian meteorites Lafayette and ALH84001 [35]. Overall, the outcrop composition could be understood as an infiltration involving martian soil and an acid–sulfate solution containing igneous mafic minerals or their leachates and weathering products.

6.2. Some candidate formation processes

The rich content of water-soluble salts in the Meridiani outcrop has caused it to be viewed in a prelim-

inary way as analogous to terrestrial evaporite deposits [6]. Careful, detailed analyses have previously predicted evaporite sequences on Mars [48] which somewhat mimic many classical sequences on Earth, in that they have major components of chlorides with alkali-element cations, carbonates with alkaline-earth cations, and relatively minor occurrences of sulfates. This scenario differs markedly from the sulfate sediments found in Meridiani Planum. A part of the difference may be explainable as a S-rich lithosphere for Mars [43] with a higher SO₃/Cl ratio in the available volatile inventory. The overwhelming large ratio of 20:1 for molar S:Cl abundance in the upper strata, and still 9:1 lower down (soils are ~5:1), illustrate the dominance of sulfate over chloride salts in this formation.

An important question about provenance of this outcrop is the scale of water involvement (“water:rock” ratio). This scale could range from a large but shallow sea, to restricted playas or springs. The widespread occurrence of characteristic bright-rimmed impact craters, now understood to reflect the presence of light-toned outcrop across large portions of Meridiani Planum [13], either argue against localized occurrences or indicate that locally generated aqueous precipitates were mixed over a broader region by aeolian processes. Given a ubiquitous source of salt from soils, the actions of aquifers, groundwater percolation, freeze/thaw of ground ice, or simply pervasive thin films of H₂O could, in principle, have produced many of these chemical signatures, especially over geologic time. Independent evidence such as diagnostic features of cross-bedding [6] implicates overland flow of H₂O in the formation of some (but not all) outcrop rocks [9]. Diagenesis to create concretions and mineral molds also requires infusions of groundwater H₂O, as discussed in McLennan et al. [8] and Tosca et al. [25].

The brines required to precipitate the salts on the surface of Mars are apparently similar in chemical composition to the relatively rare sulfate class of brines on Earth. Such Mg- or Fe-sulfate rich brines have been reported from deep wells [49], the Basque Lakes, Lake Kamloops, and Iron Mask Lake, British Columbia [50,51], Hot Lake, Washington [50]; Deadmoose Lake, Little Manitou Lake, and Freefight Lake, Saskatchewan [50,52,53]; Quero Playa Lake, central Spain [54], and Rio Tinto, Spain [55,27]. One brine from Basque Lake #2 (BQ-4 of [51]) was examined for evaporation using the computer program of Harvie et al. [56]. The simulated mineral precipitation sequence, CaCO₃–gypsum–epsomite–glauberite–bloedite–polyhalite–anhydrite–halite, is very close to the salt assemblage reported from Basque Lake #2 [51], except for the predicted minor

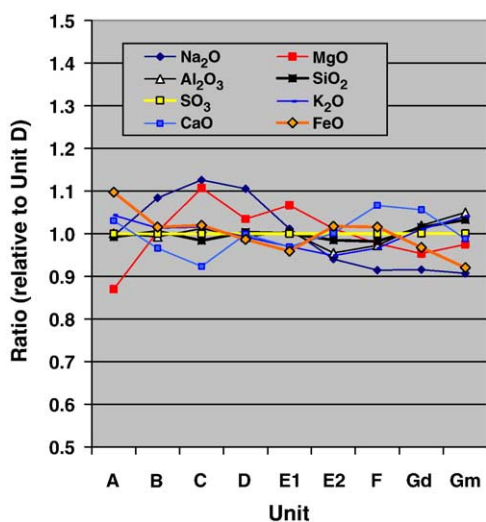


Fig. 14. Salt migration model, and element departure from a derived reference composition. Results are normalized to unit D for ease in comparison with Fig. 2.

phases glauberite and polyhalite. By simulating various Mars brines for Karatepe, we found one which produced a sequence dominated in the *final* precipitations by kieserite (52%, by mole), anhydrite (24%), and bischofite (18%), with small amounts of carnallite (2%) and halite (3%) (for a brine starting composition of $\text{SO}_4=470$, $\text{Mg}=455$, $\text{Ca}=150$, $\text{Cl}=300$, $\text{Na}=20$, and $\text{K}=10$ mM). In other calculations [25], similar but somewhat different assemblages are generated by including also the Fe chemistry and the influence of pH.

As discussed in the next section, the open questions about mobilization of salt in this outcrop are what roles five different processes may have played. These processes are water:rock ratio, evaporation, freezing, changes in pH, and shifts in oxidation potential of the environment (e.g., [25,57]).

Table 4
Amount of “mobile salt” added (+) to or depleted (–) from each unit

Unit	Salt added (%)
Tennessee (A)	4.46
Kentucky (B)	3.22
Virginia (C)	–1.77
Ontario (D)	1.77
Grindstone (E1)	–3.07
Kettlestone (E2)	0.28
Millstone (F)	–3.91
Diamond (Gd)	–7.12
MacKenzie (Gm)	–12.86
Paikia	–3.40
Wharenhui	–3.44

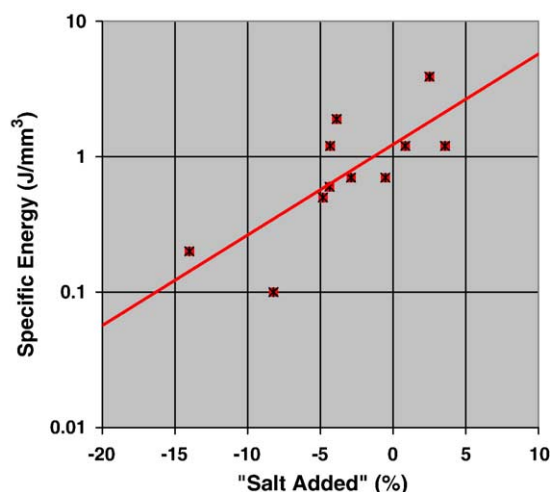


Fig. 15. Specific energies (logarithm of energy/volume) for grinding outcrop RAT holes clearly correlate with calculated content of “mobile salt” added to each sample of the Karatepe sequence. Line is LLS fit to data points.

6.3. Solubilization for mobilization

Movement of soluble Mg and Ca sulfates upward is consistent with water evaporation out the top of a saturated sediment, analogous to the formation of surface efflorescent salt crusts on Earth [58]. Migration of chloride(s) could occur via the freezing point depression mechanism during downward seepage of water under gravity. A comparative lack of vugs in the lower outcrop material [8], if true, and the suggestion that they may represent crystal molds that originally were MgCl_2 , are consistent with preferential dissolution and migration of Cl. At about 5% by volume [6], the vugs would represent an initial source of 3 to 4 wt.% of Cl, which when mobilized could supply the enrichments observed elsewhere (to 1.35 wt.% Cl). Or, a declining water table might preferentially leach NaCl downward with lesser transfer of Ca (if pH neutral) or Mg sulfates if sparse $\text{H}_2\text{O}/\text{rock}$ ratios persist. Jarosite, if present as the (K, Na)-form, could remain immobile in these scenarios because of restrictions on solubility due to pH, oxidation state, or both [25]. In many terrestrial examples, the kinetics of dissolution or precipitation of particular salts places a strong imprint on the observed deposits [59].

6.3.1. Solubility and saturation

Variations in Cl and Br concentrations could result from later diagenetic processes, including even superficial redistribution of highly soluble components by sparse quantities of solute, such as might have been provided by thin films of quasi-liquid water on grain

Table 5
Formation of reference composition from soils and SO₃/Ol/Px mixes

Component	Na ₂ O	MgO	Al ₂ O ₃	SiO ₂	P ₂ O ₅	SO ₃	Cl	K ₂ O	CaO	TiO ₂	Cr ₂ O ₃	MnO	FeO	Ni	Zn	Br
Meridiani bright soil	2.31	7.62	9.21	45.33	0.91	7.23	0.81	0.50	6.66	0.99	0.34	0.36	17.59	486	390	31
Acid volatiles					2.33	93.10	3.30	1.30							750	
Mafic component		24.83		48.15					2.21	0.98	0.73	0.39	22.70			
Calculated from components	1.54	8.54	6.14	36.91	1.06	22.91	1.18	0.58	4.75	0.80	0.33	0.29	14.89	324	405	20
Reference composition	1.55	8.48	6.15	36.94	1.06	22.93	1.16	0.59	4.84	0.78	0.20	0.32	15.01	615	401	31

surfaces even at sub-freezing temperatures [60]. Sparse H₂O availability will favor the most soluble salts, and could help explain the hyper-variability in occurrences of Br due to the very high solubility of bromides [41].

6.3.2. Temperature change and freezing

Although solubilization may have played a significant role in the initial formation of sulfate-rich sediment, subsequent wetting did not remove it to some other reservoir. Yet, differentiation into chloride and bromide-enriched regions did occur. Furthermore, some crystals were removed altogether, as evidenced by the geometrical regular vugs interpreted as mineral molds [8]. How did a highly soluble matrix of MgSO₄ persist? A possible mechanism is differential freezing point depression. Because of its heliocentric distance, Mars is today a sub-freezing planet, with average temperatures of -50 to -65 °C even in equatorial regions [61]. Excursions into temperature/pressure regimes above the freezing point of pure H₂O may have been limited or rare in both spatial and temporal extent. For the chemistries likely for Mars, significant freezing point depression by formation of brines is particularly determined by occurrences of chlorides and nitrates (if present), since the more abundant sulfates are relatively poor depressors [41,22,62,63].

Although daytime heating can transiently warm the surface of loose, insulating soil above 0 °C, the combination of annual and diurnal thermal waves is damped out just 1 or 2 dm into the regolith, especially where there is loose, fine-grained soil [61]. Chlorides of Na, Mg and Ca, and their mixtures can depress the freezing point to -20 or even -55 °C, whereas the sulfate salts considered here depress it no further than to -5 °C. Acidic species are even more effective, including the dilute aqueous sulfuric acid eutectic, H₂SO₄·9H₂O, with freezing point of -74 °C [64]. Diurnal, annual or climate-timescale temperature waves can pass through the eutectics of subsurface salt/ice mixtures without ever exceeding the triple point of pure H₂O ice. Any of these chlorides in contact with ice can enter into solution whenever the local temperature exceeds

eutectic points. By this mechanism, chlorides can migrate independently from otherwise highly soluble sulfates. The Cl-enrichment boundary at the D–E1 interface may represent the isotherm for the mineral phase responsible for transport of Cl ions to deeper zones. NaClO₄ also depresses the freezing point about the same amount as MgCl₂ (-33 °C [41]). Transport of Br separate from Cl species may occur in the form of MgBr₂, whose eutectic point is lower, at -42.7 °C [41], or along with a CaCl₂ brine, which does not fully freeze until -55 °C.

6.3.3. pH and redox change

An important question is whether the origin of the high S concentrations was in an acid environment. On earth, weathering of sulfide deposits can create acidic, sulfate-enriched waters. On Mars, the process could be more direct, especially for relatively less surface water, via magmatic outgassing. Volatiles released from magmatic intrusions or extrusive lavas include species such as S, H₂S, SO₂, SO₃, H₂SO₄, Cl₂, HCl, CO, CH₄, and CO₂, all of which are generally intrinsically acidic or are readily converted to acidic forms through oxidation by martian atmospheric UV photolysis products and subsequent reaction with H₂O vapor or liquid. Unless large quantities of liquid H₂O are available, the initial chemical weathering milieu could be expected to be highly acidic [65,26] on Mars.

Changes in deposition patterns or mobilization of Ca-sulfates requires at least slightly acidic solutions, while mobilization of K, Na-jarosite requires pH below around 3 [24,66]. Fluctuations in pH, even if temporary, could cause further selective redistribution of martian salts. That jarosite is so uniformly distributed throughout the outcrop is evidence the pH has not been very low during subsequent periods of wetting, if saturation occurred. Conversely, the fact that jarosite persists throughout outcrop rocks in substantial abundance in spite of being susceptible to slow dissolution indicates that post-depositional interactions with water, even above pH=4, have also been minimal [27,67]. Likewise, changes in oxidation po-

tential are well-known for causing precipitations in aqueous geochemical settings. Again, the uniformity of jarosite but the apparent non-uniformity of Ca-sulfates favors conditions of mildly acidic and oxidizing conditions at least at some time in the history of the formation.

7. Additional roles of water

7.1. Residual hydration states

Bound or adsorbed water in the martian surface materials was first identified based on a characteristic broad absorption feature at 3 μm in early telescopic spectra [e.g., [68]] and was subsequently observed from the Infrared Spectrometer (IRS) on Mariner 6 and 7 [69] and the Imaging Spectrometer for Mars (ISM) on Phobos [70]. Modern analysis of the IRS and ISM data sets has noted an enrichment in hydrated materials associated with all three gray hematite sites identified by the Thermal Emission Spectrometer (TES) on Mars Global Surveyor [71–73]. Increased hydration in some areas correspond with the GRS signature of hydrogen [74] and with recent OMEGA results identifying kieserite [75].

Water also has diagnostic spectral absorption features in the wavenumber range of Mini-TES. In emission most hydrated materials exhibit a narrow characteristic peak at 1650 cm^{-1} ($6.06\text{ }\mu\text{m}$), but also broad absorption from 1600 down to 1200 cm^{-1} . In Mini-TES this spectral range is also complicated by roll-off effects seen in fine particulate surfaces [76] and by lower signal-to-noise, especially at low surface temperatures (target radiance drops significantly at these high wavenumbers, shorter wavelengths). These competing effects lower the sensitivity of Mini-TES to surface hydration state and analysis is ongoing to understand these various contributions.

A survey of common evaporites, including mixed salt compounds with more than one cation, shows that about one-half of all candidate salts for Meridiani outcrops can be hydrated. Magnesium sulfate is particularly versatile, with forms ranging from one water of hydration (kieserite) up through 2, 4, 6 (hexahydrate) and even 7 water molecules per salt molecule (epsomite), which could account for significant amounts of bound H_2O in the martian regolith [62,77]. Calcium sulfate occurs commonly as gypsum, bassanite, or anhydrite, only the last of which is not hydrated. In evaporation of a sulfate-rich chloride brine in precipitation simulations [25], hydrates are predicted to figure prominently in the sequence. Hydrated Mg and Ca

sulfates have recently been detected by Mars Express [75,70,78].

We have tabulated ranges in hydration levels possible for our case 1a mineral assemblage, not including hydroxides or hydration in possible clays, serpentine, allophane or silica. The results, Table 6, show that equivalent H_2O could comprise from about 6 to 22 wt.% of this outcrop material. The value for case 2 is a minimum of 7 wt.%. Baldrige and Calvin [71] estimated that the IRS data were consistent with a local increase of 2 to 4 wt.% water in minerals at Meridiani. Measurements from the Odyssey orbiter has identified an average concentration of 7% H_2O -equivalent H down to a depth of approximately 1 m for the Meridiani Planum region [74]. Meridiani soil is estimated by us to contain 1 to 4 wt.% of H_2O of hydrated salts, so the remote sensing by neutron spectroscopy appears to be consistent with occasional exposure of outcrop in the cratered plains and etched terrain, as well as sensing below a relative thin veneer of some ten's of centimeter of soil over the layered deposits.

7.2. Astrobiology

There are numerous consequences of the outcrop salt content, its conditions of formation and subsequent environmental history that pertain to the questions of the abiotic chemical origin or life and the survival of adapted organisms. Even now, if the outcrop were to become infiltrated by liquid H_2O , it is predicted that that water would become hypersaline with soluble sulfates and chlorides. If unreacted acidity is present, there would be a low pH environment, albeit possibly transient. If Cr, Ni and Zn are soluble or extractable, they could rise to toxic levels in a brine. Hexavalent Cr is highly toxic, and a possible concern for future exploration [79]. Because Cr correlates with Fe, not S, it is unlikely to be in the

Table 6
Inferred Salt Hydration Content for Average Outcrop from Case 1a

Salt	min H_2O (%)	max H_2O (%)
$\text{MgSO}_4 \cdot 7\text{H}_2\text{O}$		14.5
$\text{MgSO}_4 \cdot \text{H}_2\text{O}$	2.8	
MgSO_4 absorbed	2.2	2.2
CaSO_4	0.0	
$\text{CaSO}_4 \cdot 2\text{H}_2\text{O}$		1.9
$\text{MgCl}_2 \cdot 6\text{H}_2\text{O}$		2.2
Na-jarosite	0.9	
H-jarosite		1.3
Hydroxylapatite		0.0
Chlorapatite	0.0	
Total H_2O	5.9	22.2

more soluble Cr^{+6} form, as it is in the Atacama [40]. Broader consideration of astrobiological implications is discussed extensively in Knoll et al. [80].

8. Conclusions and conundrums

8.1. Findings and qualifications

The Meridiani outcrops may plausibly be explained as a mix of fine-grained siliciclastic material and chemical sediments that were originally precipitated in a significant aqueous environment and have since been reworked. These sediments appear to be widespread, with a continuity in stratigraphy over the distances so far sampled. In contrast to terrestrial salt assemblages, sulfates dominate over chlorides and alkali for much of this deposit. This starting material could have been formed through elements which play a less important role. A common starting material may have been the basic combination of martian soils and known martian igneous rock chemistries, mediated by a high influx of sulfate anion. Very few major minerals, if any, may be present in their original igneous form. There does not appear to have been major infusions of liquid water, whether by infiltration or precipitation, since crater formation. Outcrops may be a repository of hydroxide and/or hydrate and hence an additional sink for sparse H_2O on Mars.

8.2. Conundrums

Current sampling may be misleading because there is abundant evidence that these are highly reworked and diagenetically altered sediments. Accordingly, it is likely that we are in an evaporite sequence that it is neither in equilibrium nor complete. For example, it cannot be ruled out that carbonate and major chloride deposits formed deeper in this sequence, or perhaps even in higher layers that have previously been eroded away by aeolian stripping. That noted, it is hazardous to speculate further on those things for which we simply have no data.

Several minerals of seemingly compatible solubility do not always associate with one another. Specifically, the variability of SO_3/Cl ratios and the hyper-variability of Br with no apparent relationship to high or low abundance of other highly soluble salts must be explained by special situations, possibly including late-stage precipitation, moisture-driven mobilization, and/or freezing point depression.

The distribution of Na and K across candidate minerals, including jarosite, is unclear. The Cl content

evidences a dichotomy, with enrichment at a zone where S concentrations begin to decrease significantly. It cannot be excluded that Br and Cl are in oxidized form, such as bromates or perchlorates, and that these forms contribute to the oxidizing power of the soils.

Acknowledgements

We wish to thank the MER Project for their indispensable support of this mission and its science. We are indebted for a significantly constructive critique of the original manuscript by D. C. Catling and also acknowledge helpful discussions with R. Quinn regarding salt minerals in the Atacama desert. This work was performed for the Jet Propulsion Laboratory, California Institute of Technology, sponsored by the National Aeronautics and Space Administration.

References

- [1] P.R. Christensen, et al., Detection of crystalline hematite mineralization on Mars by the TES: evidence for near-surface water, *J. Geophys. Res.* 105 (2000) 9623–9642.
- [2] R.E. Arvidson, F.P. Seelos, K.S. Deal, W.C. Koepfen, N.O. Snider, J.M. Kieniewicz, B.M. Hynek, M.T. Mellon, J.B. Garvin, Manteled and exhumed terrains in Terra Meridiani, Mars, *J. Geophys. Res.* 108 (ROV 14–1) (2003) 8073, doi:10.1029/2002JE001982.
- [3] R. Rieder, R. Gellert, R.C. Anderson, J. Brückner, B.C. Clark, G. Dreibus, T. Economou, G. Klingelhöfer, G.W. Lugmair, D.W. Ming, S.W. Squyres, C. d'Uston, H. Wänke, A. Yen, J. Zipfel, Chemistry of rocks and soils at Meridiani Planum from the alpha particle X-ray spectrometer, *Science* 306 (2004) 1746–1749.
- [4] G. Klingelhöfer, R.V. Morris, B. Bernhardt, C. Schröder, D.S. Rodionov, P.A. de Souza Jr., A. Yen, R. Gellert, E.N. Evlanov, B. Zubkov, J. Foh, E. Kankeleit, P. Gütlich, D.W. Ming, R. Renz, T. Wdowiak, S.W. Squyres, R.E. Arvidson, Jarosite and hematite at Meridiani Planum from the Mössbauer spectrometer on the Opportunity rover, *Science* 306 (2004) 1740–1745.
- [5] P.R. Christensen, M.B. Wyatt, T.D. Glotch, A.D. Rogers, S. Anwar, R.E. Arvidson, J.L. Bandfield, D.L. Blaney, C. Budney, W.M. Calvin, A. Fallacaro, R.L. Fergason, N. Gorelick, T.G. Graff, V.E. Hamilton, A.G. Hayres, J.R. Johnson, A.T. Knudson, H.Y. McSween Jr., G.L. Mehall, L.K. Mehall, J.E. Moersch, R.V. Morris, M.D. Smith, S.W. Squyres, S.W. Ruff, M.J. Wolff, Mineralogy at Meridiani Planum from the Mini-TES Experiment on the Opportunity Rover, *Science* 306 (2004) 1733–1739, doi:10.1126/science.1104909.
- [6] S.W. Squyres, J.P. Grotzinger, R.E. Arvidson, J.F. Bell III, P.R. Christensen, B.C. Clark, J.A. Crisp, W.H. Farrand, K.E. Herkenhoff, J.R. Johnson, G. Klingelhöfer, A.H. Knoll, S.M. McLennan, H.Y. McSween Jr., R.V. Morris, J.W. Rice Jr., R. Rieder, L.A. Soderblom, In situ evidence for an ancient aqueous environment on Mars, *Science* 306 (2004) 1709–1714.
- [7] R. Gellert, et al., APXS Results for the Opportunity Rover at Meridiani Planum, *J. Geophys. Res.* (in press).
- [8] S.M. McLennan, et al., Provenance and diagenesis of sedimentary rocks in the vicinity of the Opportunity landing site, Mer-

- idiani Planum, Mars, Earth Planet. Sci. Lett. 240 (2005) 95–121. (this issue).
- [9] J.P. Grotzinger et al., Stratigraphy and sedimentology of a dry to wet eolian depositional system, Burns formation, Meridiani Planum, Mars, Meridiani Planum Earth Planet. Sci. Lett. 240 (2005), 11–72. (this issue).
- [10] R.V. Morris, et al., Mineralogy at Gusev crater from the Mössbauer spectrometer on the Spirit rover, Science 305 (2004) 833–836.
- [11] B.C. Clark, A.K. Baird, R.J. Weldon, D.M. Tsusaki, L. Schnabel, M.P. Candelaria, Chemical composition of Martian fines, J. Geophys. Res. 87 (1982) 10,059–10,067.
- [12] R. Gellert, R. Reider, R.C. Anderson, J. Brueckner, B.C. Clark, G. Dreibus, T. Economou, G. Klingelhofer, G.W. Lugmair, D.W. Ming, S.W. Squyres, C. d'Uston, H. Waenke, A. Yen, J. Zipfel, Chemistry of rocks and soils in Gusev Crater from the alpha particle X-ray spectrometer, Science 305 (2004) 829–832.
- [13] M. Malin, personal communication, 2004.
- [14] J. Brückner, et al., Hematite pigmentation of the surface of Meridiani Planum and on basaltic rocks in Gusev crater, LPSC XXXV (2005) (extended abstract submitted).
- [15] J. Brückner, G. Dreibus, E. Jagoutz, R. Gellert, G. Lugmair, R. Rieder, H. Wänke, J. Zipfel, G. Klingelhofer, B.C. Clark, D.W. Ming, A. Yen, K.E. Herkenhoff, Hematite on the surface of Meridiani Planum and Gusev crater, in: Lun. Planet. Sci. Conf., vol. XXXVI (2005) p. 1767.
- [16] A.S. Yen, et al., An integrated view of the chemistry and mineralogy of martian soils, Nature 436 (2005) 49–54, doi:10.1038/nature03637.
- [17] B.C. Clark, Geochemical components in Martian soil, Geochim. Cosmochim. Acta 57 (1993) 4575–4581.
- [18] J.L. Bandfield, Global mineral distributions on Mars, J. Geophys. Res. 107 (E6) (2002) 5042, doi:10.1029/2001JE001510.
- [19] E.Z. Noe Dobrea, J.F. Bell III, M.J. Wolff, K.D. Gordon, H₂O and OH-bearing minerals in the martian regolith: analysis of 1997 observations from HST/NICMOS, Icarus 166 (2003) 1–20.
- [20] P.R. Christensen, S.W. Ruff, The formation of the hematite-bearing unit in Meridiani Planum: evidence for deposition in standing water, J. Geophys. Res. 109 (2004) E08003, doi:10.1029/2003JE002233.
- [21] H.Y. McSween, et al., Basaltic rocks analyzed by the Spirit rover in Gusev crater, Science 305 (2004) 842–845.
- [22] B.C. Clark, D. van Hart, The salts of Mars, Icarus 45 (1981) 370–378.
- [23] S.M. McLennan, Chemical composition of martian soil and rocks: complex mixing and sedimentary transport, Geophys. Res. Lett. 27 (2000) 1335–1338.
- [24] R.G. Burns, Weathering of ferromagnesian minerals on Mars, Geochim. Cosmochim. Acta 57 (1993) 4555–4574.
- [25] N.J. Tosca et al., Geochemical modeling of evaporation processes on Mars: insight from the sedimentary record at Meridiani Planum, Earth Planet. Sci. Lett. 240 (2005) 122–148. (this issue).
- [26] A. Banin, F.X. Han, I. Kan, A. Cicelsky, Acidic volatiles and the Mars soil, J. Geophys. Res. 102 (1997) 13,341–13,356.
- [27] D.C. Fernandez-Remolar, R.V. Morris, J.E. Gruener, R. Amils, A.H. Knoll. The Río Tinto Basin, Spain: mineralogy, sedimentary geobiology, and implications for interpretation of outcrop rocks at Meridiani Planum, Mars, Earth Planet. Sci. Lett. 240 (2005) 149–167. (this issue).
- [28] R.V. Morris, D.C. Golden, J.F. Bell III, T.D. Shelfer, A.C. Scheinost, N.W. Hinman, G. Furniss, S.A. Mertzman, J.L. Bishop, D.W. Ming, C.C. Allen, D.T. Britt, Mineralogy, composition, and alteration of Mars Pathfinder rocks and soils: evidence from multispectral, elemental, and magnetic data on terrestrial analogue, SNC meteorite, and Pathfinder samples, J. Geophys. Res. 105 (2000) 1757–1817.
- [29] B. Jakosky, B. Henderson, M. Mellon, Chaotic obliquity and the nature of the martian climate, J. Geophys. Res. 100 (1995) 1579–1584.
- [30] J. Pollack, J. Kasting, S. Richardson, K. Poliakoff, The case for a wet, warm climate on early Mars, Icarus 71 (1987) 203–224.
- [31] R.E. Stevens, M.K. Carron, Simple field test for distinguishing minerals by abrasion pH, Am. Mineral. 1–2 (1948) 31–49.
- [32] B.C. Clark, S.L. Kenley, D.L. O'Brien, G.R. Huss, R. Mack, A.K. Baird, Heterogeneous phase reactions of martian volatiles with putative regolith minerals, J. Mol. Evol. 14 (1979) 91–102.
- [33] M.G. Siemann, M. Schramm, Henry's and non-Henry's law behavior of Br in simple marine systems, Geochim. Cosmochim. Acta 66 (2002) 1387–1399.
- [34] D.J. Bottomley, D.C. Gregoire, K.G. Raven, Saline groundwaters and brines in the Canadian Shield: geochemical and isotopic evidence for a residual evaporite brine component, Geochim. Cosmochim. Acta 58 (1994) 1483–1498.
- [35] K. Lodders, A survey of shergottite, nakhlite and chassigny meteorites whole-rock compositions, Meteorit. Planet. Sci. 33 (1998) A183–A190.
- [36] H.E. Newsom, J.J. Hagerty, Chemical components of the martian soil: melt degassing, hydrothermal alteration, and chondritic debris, J. Geophys. Res. 102 (1997) 19,345–19,355.
- [37] D.M. Hunten, Possible oxidant sources in the atmosphere and surface of Mars, J. Mol. Evol. 14 (1979) 71–78.
- [38] Y.L. Yung, W.B. DeMore, Photochemistry of Planetary Atmospheres, Oxford Univ. Press, NY, 1999.
- [39] V.I. Oyama, B.J. Berdahl, The Viking gas exchange experiment results from Chryse and Utopia surface samples, J. Geophys. Res. 82 (1977) 4669–4676.
- [40] G.E. Erickson, Geology and origin of the Chilean nitrate deposits, Geol. Surv. Prof. Pap. 1188 (1981).
- [41] W. Linke, Solubilities of Inorganic and Metal Organic Compounds, 4th edition, Am. Chem. Soc., Washington DC, 1965.
- [42] H. Wänke, J. Brückner, G. Dreibus, R. Rieder, I. Ryabchikov, Chemical composition of rocks and soils at the Pathfinder site, Space Sci. Rev. 96 (2001) 317–330.
- [43] B.C. Clark, A.K. Baird, Is the Martian lithosphere sulfur rich? J. Geophys. Res. 84 (1979) 8395–8402.
- [44] L.A. Haskin, et al., Water alteration of rocks and soils from the Spirit rover site, Gusev crater, Mars, Nature 436 (2005) 66–69, doi:10.1038/nature03640.
- [45] D.J. Des Marais, B.C. Clark, L.S. Crumpler, J.D. Farmer, J.P. Grotzinger, L.A. Haskin, A.H. Knoll, G.A. Landis, J. Moersch, C. Schröder, T. Wdowiak, A.S. Yen, D. Blaney, N.A. Cabrol, A.G. Hayes, J. Rice, S.W. Squyres, Astrobiological perspectives on the basaltic plains in Gusev crater, Nature (in preparation).
- [46] G. Dreibus, E. Jagoutz, B. Spettel, H. Wänke, Phosphate-mobilization on Mars? Implications from leach experiments on SNCs, LPSC XXVII (1996) 323 (extended abstract).
- [47] J.L. Bandfield, T.D. Glotch, P.R. Christensen, Spectroscopic identification of carbonate minerals in the martian dust, Science 301 (2003) 1084–1087.

- [48] D.C. Catling, A chemical model for evaporites on early Mars: possible sedimental tracers of the early climate and implications for exploration, *J. Geophys. Res.* 104 (1999) 16,453–16,469.
- [49] D.E. White, J.D. Hem, G.A. Waring, Data of geochemistry, chapter F — chemical composition of subsurface waters, U. S. Geol. Surv. Prof. Pap. 440-F (1963).
- [50] D.A. Livingstone, Chemical composition of rivers and lakes, U. S. Geol. Surv. Prof. Pap. 440-G (1963)1994 (64 pp.).
- [51] H.W. Nesbitt, Groundwater evolution, authigenic carbonates and sulfates, of the Basque Lake No. 2 basin, Canada, in: R.J. Spencer, I.-M. Chou (Eds.), *Fluid-Mineral Interactions: A Tribute to H.P. Eugster*, Special Publication, vol. 2, Geochemical Society, 1990, pp. 355–371.
- [52] W.L. Last, Deep-water evaporite mineral formation in lakes of western Canada, in: R.W. Renaut, W.M. Last (Eds.), *Sedimentology and Geochemistry of Modern and Ancient Saline Lakes*, Society for Sedimentary Geology Special Publication, vol. 50, 1994, pp. 51–59.
- [53] W.B. Lyons, M.E. Hines, W.M. Last, R.M. Lent, Sulfate reduction rates in microbial mat sediments of differing chemistries: implications for organic carbon preservation in saline lakes, in: R.W. Renaut, W.M. Last (Eds.), *Society for Sedimentary Geology Special Publication*, vol. 50, 1994, pp. 13–20.
- [54] S. Ordóñez, S.S. Moral, M.G. Del Cura, E.R. Badiola, Precipitation of salts from Mg^{2+} -(Na^+)- SO_4 -Cl-playa-lake brines: the endorheic saline ponds of La Mancha, central Spain, in: R.W. Renaut, W.M. Last (Eds.), *Sedimentology and Geochemistry of Modern and Ancient Saline Lakes*, Society for Sedimentary Geology Special Publication, vol. 50, 1994, pp. 61–71.
- [55] F.G. Ferris, L. Hallbeck, C.B. Kennedy, K. Pedersen, Geochemistry of acidic Rio Tinto headwaters and role of bacteria in solid phase metal partitioning, *Chem. Geol.* 212 (2004) 291–300.
- [56] C.E. Harvie, N. Møller, J.H. Weare, The prediction of mineral solubilities in natural waters: the Na K Mg Ca-H-Cl-SO₄ OH-HCO₃-CO₃-CO₂-H₂O system to high ionic strengths at 25 °C, *Geochim. Cosmochim. Acta* 48 (1984) 723–751.
- [57] G.M. Marion, D.C. Catling, J.S. Kargel, Modeling aqueous ferrous iron chemistry at low temperatures with application to Mars, *Geochim. Cosmochim. Acta* 67 (2003) 4251–4266.
- [58] J.P. Smoot, T.K. Lowenstein, Depositional environments of non-marine evaporites, in: J.L. Melvin (Ed.), *Evaporites, Petroleum and Mineral Resources*, Elsevier Developments in Sedimentology, vol. 50, Elsevier, Amsterdam, 1991, pp. 189–347.
- [59] Peter Sonnenfeld, *Brines and Evaporites*, Academic Press, Inc., New York, 1984.
- [60] D.M. Anderson, L.W. Gatto, F.C. Ugolini, Ion mobility at low temperatures, *Antarct. J.* 30 (1972) 114–116.
- [61] H.H. Kieffer, T.Z. Martih, A.L.R. Peterfreund, B.M. Jakosky, Thermal and albedo mapping of Mars during the Viking primary mission, *J. Geophys. Res.* 82 (1977) 4249–4291.
- [62] B.C. Clark, Implications of abundant hygroscopic minerals in the Martian regolith, *Icarus* 34 (1978) 645–665.
- [63] G.W. Brass, The stability of brines on Mars, *Icarus* 42 (1980) 20–28.
- [64] S.T. Martin, Phase transitions of aqueous atmospheric particles, *Chem. Rev.* 100 (2000) 3403–3453.
- [65] A.K. Baird, B.C. Clark, On the original igneous source of Martian fines, *Icarus* 45 (1981) 113–123.
- [66] D.C. Catling, On Earth, as it is on Mars? *Nature* 429 (2004) 707–708.
- [67] M.E.E. Madden, R.J. Bodnar, J.D. Rimstidt, Jarosite as an indicator of water-limited chemical weathering on Mars, *Nature* 431 (2004) 821–823.
- [68] J.R. Houck, J.B. Pollack, C. Sagan, D. Schaack, J.A. Decker Jr., High altitude infrared spectroscopic evidence for bound water on Mars, *Icarus* 18 (1973) 470–480.
- [69] G.C. Pimentel, P.B. Forney, K.C. Herr, Evidence about hydrate and solid water in the Martian surface from the 1969 Mariner infrared spectrometer, *J. Geophys. Res.* 79 (1974) 1623–1634.
- [70] J.-P. Bibring, et al., Results from the ISM experiment, *Nature* 341 (1989) 591–593.
- [71] A.M. Baldridge, W.M. Calvin, Hydration state of the Martian coarse-grained hematite exposures: implications for their origin and evolution, *J. Geophys. Res.* 109 (2004) E04S90, doi:10.1029/2003JE002066.
- [72] W. Calvin, A. Fallacaro, A. Baldridge, Synthesis of Spectral Data From the Grey Hematite Regions of Mars, AGU, 2003, Fall.
- [73] W. Calvin, A. Fallacaro, A. Baldridge, Synthesis of spectral data from the grey hematite regions of Mars, *Eos Trans. AGU* 84 (46) (2003) (Fall Meet. Suppl., Abstract P12C-04).
- [74] W.C. Feldman, et al., Global distribution of near-surface hydrogen on Mars, *J. Geophys. Res.* 109 (2004) E09006, doi:10.1029/2003JE002160.
- [75] A. Gendrin, N. Mangold, J.-P. Bibring, Y. Langevin, B. Gondet, F. Poulet, G. Bonello, C. Quantin, J. Mustard, R. Arvidson, S. LeMouélic, Sulfates in Martian Layered Terrains: the OMEGA/Mars Express View, *Science* 30 (2005) 1587–1591, doi:10.1126/science.1109087.
- [76] S.W. Ruff, P.R. Christensen, Bright and dark regions on Mars: particle size and mineralogical characteristics based on Thermal Emission Spectrometer data, *J. Geophys. Res.* 107 (E12) (2002) 5119, doi:10.1029/2001JE001580.
- [77] D.T. Vaniman, D.L. Bish, S.J. Chipera, C.I. Fialips, J.W. Carey, W.C. Feldman, Magnesium sulphate salts and the history of water on Mars, *Nature* 431 (2004) 663–665.
- [78] J.-P. Bibring, Y. Langevin, A. Gendrin, B. Gondet, F. Poulet, M. Berthé, A. Soufflot, R. Arvidson, N. Mangold, J. Mustard, P. Drossart, Mars surface diversity as revealed by the OMEGA/Mars Express observations, *Science* 307 (2005) 1576–1581, doi:10.1126/science.1108806.
- [79] F.H. Hauck, H.Y. McSween, D.H. Bennett, C. Breazeal, B.C. Clark, V.R. Eshleman, J. Haas, J.B. Reid, J. Richmond, R.E. Turner, W.L. Whittaker, *Safe on Mars: Precursor Measurements Necessary to Support Human Operations on the Martian Surface*, National Academy Press, Washington, DC, 2002.
- [80] A.H. Knoll, et al., An astrobiological perspective on Meridiani Planum, *Earth Planet. Sci. Lett.* 240 (2005) 179–192. (this issue).